

Point-proton density distributions of stable nuclei

Tian Yu Wu,¹ Bao Hua Sun,^{1,*} Hui Hui Xie,² Jun Yao Xu,¹ and Ge Guo¹

¹*School of Physics, Beihang University, Beijing 100191, China*

²*College of Physics, Jilin University, Changchun 130012, China*

(Dated: May 9, 2025)

Abstract

Point-proton density distributions are deduced for 130 stable nuclei from ^7Li to ^{232}Th from nuclear charge densities determined in elastic electron scattering. There are 171 cases presented in model-dependent forms, including the modified Harmonic-oscillator function, two-parameter Fermi function (2pF), three-parameter Fermi function, three-parameter Gaussian function, and 97 in Fourier-Bessel series model-independent forms. Independent of density functions, the point-proton root-mean-square (rms) radii of the derived point-proton density show excellent agreement with each other. We identify cases where the tabulated data of charge densities and charge radii are inconsistent, and the deduced point-proton density distributions are inaccurate due to insufficient experimental momentum transfer coverage or inconsistent scattering experiments. For the widely used 2pF distribution, it is found that the surface diffuseness parameters can be empirically calculated from those of charge density, while the half-density radius parameters follow the $A^{1/3}$ rule. The derived point-proton density distributions can be used as input in nuclear reaction studies and compared with nuclear model predictions.

*Electronic address: bhsun@buaa.edu.cn

Contents

I. Introduction	2
II. Derivation of the Point-proton density distribution	3
A. Overview of nuclear charge density data	3
B. Charge density distributions in different forms	6
C. Unfolding charge density distributions	6
III. results and discussion	9
A. Accuracy of point proton rms radii	9
B. Two-parameter Fermi point-proton densities	13
C. Point-proton densities for ^{48}Ca and ^{208}Pb	15
IV. summary	16
Acknowledgments	17
Model-dependent and model-independent densities distribution	18
Explanation of Tables	20
References	55

I. INTRODUCTION

In the study of nuclei—finite quantum systems with diffuse boundaries—the point-proton density distribution (ρ_p) plays a fundamental role. It not only captures the overall size and detailed internal distribution of protons but also serves as a cornerstone for defining key physical quantities, such as point-proton root-mean-square (rms) radii ($\langle r^2 \rangle_p^{1/2}$). In addition, it is also an indispensable input for nuclear reaction models to link nuclear structure with reaction mechanisms. A systematic study of the nucleon density distributions of finite nuclei is important for understanding the isospin dependence of the nuclear many-body system.

Experimentally, point-proton density distributions have been extracted through proton elastic scattering [1–3] and heavy ions reactions [4–6]. However, utilizing the hadronic

probes is challenging due to the interplay between the nuclear structure and the reaction dynamics governed by the strong force. On the other hand, electromagnetic probes that are well-understood by quantum electrodynamics (QED) have been employed for measuring the charge density distribution (ρ_c). On the order of the fine-structure constant $\alpha=1/137$, the weakly interacting nature between the electron and target nuclei prevents disruption of the target nuclei. Being a useful technique for studying nuclear structure [7–9], elastic electron scattering remains the sole method for ascertaining the charge density distribution ρ_c within a nucleus. Until now, elastic electron scattering experiments have targeted almost all the stable nuclei [10, 11]. Recently, the electron scattering has been successfully extended to unstable nuclei [12].

Nuclear charge density distribution is primarily determined by the distribution of point protons inside an atomic nuclide. This work aims to provide a consistent database of point-proton density distributions for stable isotopes from elastic electron scattering experiments. This database can serve as a basic input for nuclear reaction models and examinations for nuclear structure models. For this purpose, the point-proton densities are derived in different forms neglecting the contribution of spin-orbital density. The point-neutron density (ρ_n) is assumed to be $\rho_n = \frac{N}{Z} \rho_p$.

This paper is organized as follows. In Sec . II, we will survey the charge density data, compare different density distribution forms, and present the details of the ρ_p deduction procedure. In Sec. III, we discuss the deduced ρ_p compared to ρ_c , the precisions in point-proton rms radii and ρ_p for ^{48}Ca and ^{208}Pb . Finally, the conclusion is given in Sec . IV.

II. DERIVATION OF THE POINT-PROTON DENSITY DISTRIBUTION

A. Overview of nuclear charge density data

In elastic electron scatterings, the differential cross sections $\frac{d\sigma}{d\Omega}$ are connected to the nuclear response, the charge form factor (F_c). It is the Fourier component of the charge density distribution at a specific momentum transfer, q , in the framework of plane-wave impulse approximation (PWIA) [8, 13]. Owing to the dependence of the Mott cross section on $1/q^4$, the determination of F_c , in reality, has to be measured in a limited range of momentum transfer. This necessitates employing a phenomenological model to parameterize

the charge density distribution effectively. The “experimental” charge densities [10, 11] have been tabulated in model-dependent forms, including the Harmonic-oscillator function (HO), Modified Harmonic-oscillator function (MHO), two-parameter Fermi function (2pF), three-parameter Fermi function (3pF), three-parameter Gaussian function (3pG), model-independent analyses of Sum-of-Gaussian function (SOG) [14] and Fourier-Bessel (FB) [15]. The explicit expressions are given in the Appendix IV.

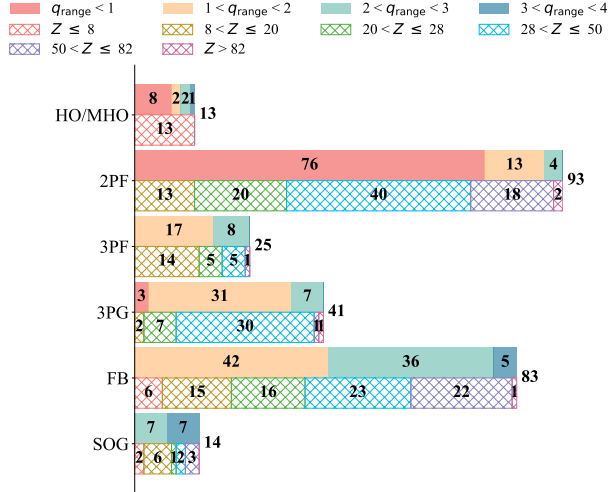


FIG. 1: Classification of charge density data in Refs. [10, 11] by the density distribution models, the momentum transfer ranges covered and the proton numbers (Z). Shown in each category is the number of cases. Note that there are cases where various experiments exist for the same nucleus.

Charge density distribution parameters and charge radii were compiled for 136 stable nuclei from ^3H to ^{238}U in Refs. [10, 11]. All the ρ_c data are categorized in Fig. 1 according to the momentum transfer range (q_{range}) covered experimentally and the proton numbers of relevant nuclides. A significant portion of the charge density data expressed in HO/MHO and 2pF forms corresponds to q_{range} of less than 1 fm^{-1} . In this case, the form factor covering the first maximum can help to evaluate the gross size and shape of ρ_c . For 3pF and 3pG forms, the additional inner depth parameter offers more details of the density distributions. The form factors often reach the second minimum, with most q_{range} lying between 1 and 2 fm^{-1} . For the model-independent distributions, a larger q_{range} is typically required to look into the details of the central region of the density. As elucidated in Fig. 1, nearly half of the FB data, namely 41 out of 83, are measured with q_{range} between 2 and 4 fm^{-1} , while the remaining data have q_{range} less than 2 fm^{-1} . For the latter, the $q^{-4} \exp(-q^2 r_p^2)$ dependence is

assumed for F_c beyond the experiment accessible data [10, 15], where r_p^2 is the mean-square charge radii of a proton.

For the p -shell nuclei, the simple model-dependent density forms, HO and MHO, are usually employed as an effective approximation. The most adapted 2pF form has been used to describe nuclei heavier than oxygen, together with 3pF and 3pG. To avoid model dependency, model-independent distributions, SOG, and FB are introduced. In particular, 83 cases in FB form are supposed to be “ideal” charge density data. It is worth noting that different experiments exist for one nucleus. We noticed some data exhibit inconsistencies, as the rms charge radii $\langle r^2 \rangle_c^{1/2}$ tabulated in Refs. [10, 11] deviate from those calculated with the tabulated density parameters. The data with radii deviations over 0.01 fm are listed in Table I.

TABLE I: Inconsistent data in Refs. [10, 11]. Shown are the specific nuclide, charge density distribution form, the tabulated rms charge radii ($\text{table} \langle r^2 \rangle_c^{1/2}$), the calculated rms charge radii ($\text{cal} \langle r^2 \rangle_c^{1/2}$) using the tabulated charge densities and the deviation of the above two.

Nucleus	Model	$\text{table} \langle r^2 \rangle_c^{1/2}$ (fm)	$\text{cal} \langle r^2 \rangle_c^{1/2}$ (fm)	Deviation (fm)
^{20}Ne	3pF	2.992 ^a	2.949	0.043
^{24}Mg	3pF	2.985 ^a	2.956	0.029
^{25}Mg	3pF	3.003 ^a	2.982	0.021
^{28}Si	3pF	3.086 ^a	3.076	0.01
^{48}Ti	2pF	3.713 ^a	3.693	0.02
^{59}Co	3pG	3.775 ^a	3.629	0.146
^{89}Y	2pF	4.24 ^a	4.254	0.014
^{96}Zr	3pG	4.396 ^a	4.371	0.025
^{93}Nb	2pF	4.31 ^a	4.332	0.022
^{74}Se	2pF	4.07 ^b	4.081	0.011
^{74}Se	3pG	4.04 ^b	4.131	0.091
^{76}Se	3pG	4.133 ^b	4.212	0.079
^{78}Se	3pG	4.111 ^b	4.196	0.085
^{82}Se	3pG	4.122 ^b	4.18	0.058

^aFrom dataset [10].

^bFrom dataset [11].

B. Charge density distributions in different forms

For 75 cases out of 136 nuclei in the data compilations, different charge densities have been extracted from different experiments for one single nuclide. One such case is ^{116}Sn . In Fig. 2 (a), the charge densities of ^{116}Sn are presented in three different forms, i.e., the model-independent SOG [16] with 12 free parameters, the model-dependent 2pF [17] and 3pG [18] models. The error bands for 2pF and 3pF are also indicated. For SOG, no uncertainties are given in the original literature.

In contrast to the uniform distribution of the 2pF model, the SOG displays a central density resembling a “wine bottle”. The differences among the three densities start to reduce at the shoulder region and become hardly discernible at the tail region. Although 2pF and 3pG cannot reproduce the details in the central area, they can give consistent $\langle r^2 \rangle_c^{1/2}$ and $\langle r^4 \rangle_c$ values within experiment uncertainties as seen in Fig. 2 (b) and (c).

In Fig. 2 (d), the charge form factors F_c are presented for the three types of densities. High-momentum transfer scattering explores the internal density distribution of the nucleus, whereas low-momentum transfer focuses on the surface area. In contrast to the SOG model, the 2pF and 3pG form factors begin to deviate significantly when $q > 2.5 \text{ fm}^{-1}$, highlighting their limitations in representing the central density. The least range of q would ensure 2pF and 3pG to characterize the nucleus bulk and shape, but it is risky to extend 2pF and 3pG form factors to the q_{range} beyond experiments. Therefore, one should note that ρ_p should be deduced in the same q_{range} as the experiment covered.

C. Unfolding charge density distributions

The nuclear charge density distribution in the momentum space F_c , is written as [19]

$$F_c(\mathbf{q}) = \sum_{\tau \in \{p,n\}} [G_{E\tau}(\mathbf{q}^2)F_\tau(\mathbf{q}) + F_{2\tau}(\mathbf{q}^2)F_{W\tau}(\mathbf{q})], \quad (1)$$

where F_τ and $F_{W\tau}$ ($\tau \in \{p,n\}$) are the Fourier transform of point-nucleon density and the spin-orbit density [20, 21], respectively. $\mathbf{q}^2 \equiv -q_\mu q^\mu$, where q_μ is the momentum transfer. The quantities $G_{E\tau}$ and $F_{2\tau}$ are the nucleon’s electric Sachs and Pauli form factors, respectively.

The parameterization of nucleon form factors adopted in this work are taken from

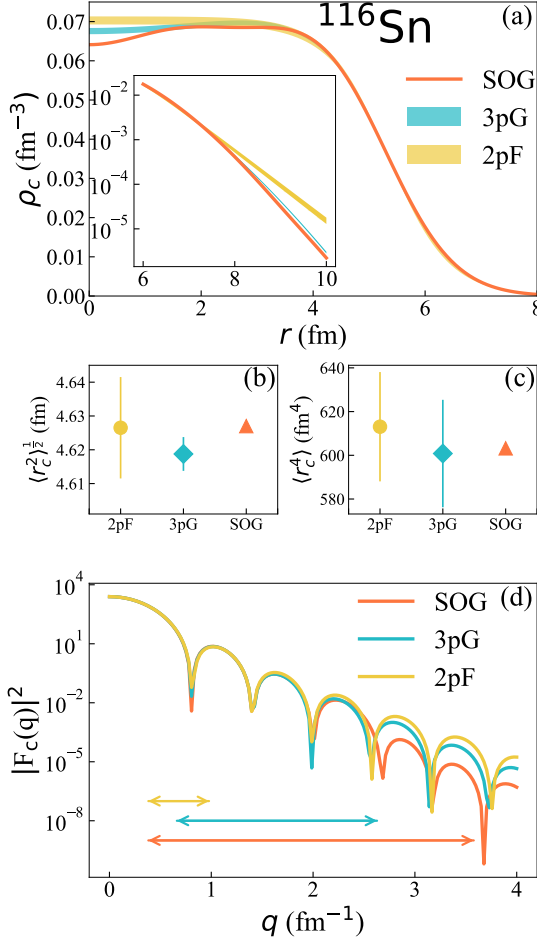


FIG. 2: (a) Comparison of ρ_c of ^{116}Sn measured in different experiments in Ref. [10] with three function types: 2pF (blue line), 3pG (orange line), and SOG (red line). The inset shows the densities at the tail region. The relevant rms radii (b) and fourth-order moment (c) of three densities are also given. (d) The corresponding form factor F_c is deduced from ρ_c . Arrows represent the momentum transfer regions covered in the experiments.

Ref. [22],

$$G_{Ep}(q^2) = \frac{1}{(1 + r_p^2 q^2 / 12)^2}, \quad (2)$$

$$G_{En}(q^2) = \frac{1}{(1 + r_+^2 q^2 / 12)^2} - \frac{1}{(1 + r_-^2 q^2 / 12)^2},$$

where the proton charge radius $r_p = 0.8414$ fm [23] and $r_\pm^2 = r_{av}^2 \pm \frac{1}{2}r_n^2$, where $r_{av}^2 = 0.81$ fm 2 is the average of the squared radius for positive and negative charge distributions and $r_n^2 = -0.11$ fm 2 [24] is the mean-square radius of the neutron.

The nuclear charge density can be derived from the inverse Fourier transformation of the

nuclear charge form factor, and is written in the relativistic form as:

$$\rho_c(r) = \sum_{\tau \in \{p,n\}} [\rho_{c\tau}(r) + W_{c\tau}(r)], \quad (3)$$

where

$$\rho_{c\tau}(r) = \frac{1}{r} \int_0^\infty dx x \rho_\tau(x) [g_\tau(|r-x|) - g_\tau(r+x)], \quad (4)$$

$$W_{c\tau}(r) = \frac{1}{r} \int_0^\infty dx x W_\tau(x) [f_{2\tau}(|r-x|) - f_{2\tau}(r+x)]. \quad (5)$$

Here, $\rho_\tau(x)$ and $W_\tau(x)$ are the nucleon and spin-orbit density. The functions $g_\tau(x)$ and $f_{2\tau}(x)$ are the Fourier transforms of Sachs and Pauli form factors, respectively. The charge density depends on the point-proton and point-neutron density, the proton and neutron spin-orbit densities, and the single-proton and single-neutron charge densities.

The corresponding mean-square radius of nuclear charge density for the nuclide (Z, N), $\langle r^2 \rangle_c$, is given by [25]

$$\langle r^2 \rangle_c = \langle r^2 \rangle_p + r_p^2 + \langle r^2 \rangle_{W_p} + \frac{N}{Z} (r_n^2 + \langle r^2 \rangle_{W_n}), \quad (6)$$

where Z and N are the number of protons and neutrons, respectively. The term $\langle r^2 \rangle_p$ is the point-proton mean-square radius. The terms $\langle r^2 \rangle_{W_p}$ and $N/Z \langle r^2 \rangle_{W_n}$ represent the proton and neutron spin-orbit contributions, respectively. Due to the proton charge radius puzzle [26], adopting the alternative value of $r_p = 0.88$ fm would lead to a difference in $\langle r^2 \rangle_p^{1/2}$ of approximately $0.0688/(2\langle r^2 \rangle_c^{1/2}) \approx 0.0688/(2.4A^{1/3})$ fm, *i.e.*, 0.015 fm for $A \leq 10$, and 0.006 fm for $A \approx 200$. The differences are generally smaller or comparable to experimental uncertainties. The deduced ρ_p is insensitive to the selection of r_p .

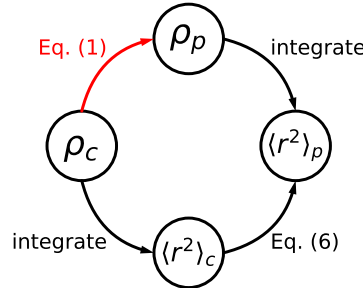


FIG. 3: Relationship of charge density distribution (ρ_c), point-proton density distribution (ρ_p), mean-square charge radii ($\langle r^2 \rangle_c$) and mean-square point-proton radii ($\langle r^2 \rangle_p$).

In Fig. 3, ρ_c , ρ_p , $\langle r^2 \rangle_c$ and $\langle r^2 \rangle_p$ are illustrated with equations interconnected. This work aims to provide systematic point-proton density distributions deduced from ρ_c , as indicated by the red arrow. The unique $\langle r^2 \rangle_p$ value can be calculated from Eq. (6) or from integrating the deduced ρ_p . Naturally, the deviations in $\langle r^2 \rangle_p$ between the two ways point to the accuracy of computing ρ_c to ρ_p .

Note that the original F_c data is often missing from the literature. Instead, the tabulated ρ_c is employed to deduce F_c in this work. The point-proton densities are deduced from the corresponding charge densities, which are parameterized in the same form. For ρ_c in the FB and SOG forms, we deduce ρ_p in the FB form. For a systematic study, we provide ρ_p in the 2pF form for all the ρ_c data in the 2pF, 3pF, 3pG, FB, and SOG forms.

The free parameters in ρ_p are determined by fitting F_c with the nonlinear least-squares method [27]. The q_{range} is fixed in the same way as covered in electron scattering. The point-neutron density ρ_n is assumed to be $\frac{N}{Z}\rho_p$ [28]. We have examined the impact of the neutron skin effect by taking ^{48}Ca , ^{116}Sn , and ^{208}Pb as examples, which have known $\langle r^2 \rangle_n^{1/2}$ [2, 3, 29]. We found it has minimal effect on $\langle r^2 \rangle_p^{1/2}$ and ρ_p . One should note that the spin-orbit densities of neutrons and protons have opposite signs, thus partially offset each other in the overall contribution [19]. For the above reason, the contribution of spin-orbit densities is neglected, so that $\langle r^2 \rangle_{W_p}$ and $N/Z\langle r^2 \rangle_{W_n}$ are thrown out of Eq. (6).

Point-proton density distributions are deduced from over 200 charge densities for 136 stable nuclei [10, 11]. Among them, 13 ρ_c cases are parameterized in HO/MHO, 93 in 2pF, 25 in 3pF, 40 in 3pG, 83 in FB, and 14 in SOG. All the derived ρ_p parameters and radii are listed in Tables III and IV.

III. RESULTS AND DISCUSSION

A. Accuracy of point proton rms radii

The radius differences $\Delta\langle r^2 \rangle_p^{1/2}$ between the rms point-proton radii from the derived ρ_p (hereafter as ${}^2\langle r^2 \rangle_p^{1/2}$) and that from Eq. (6) (hereafter as ${}^1\langle r^2 \rangle_p^{1/2}$), are presented as violin and box plots in Fig. 4 (a). The results are categorized based on different types of distribution functions. The box represents the range in which the middle 50% of the data lies. The lower and upper edge of the box corresponds to the first quartile (Q1) and the third quartile

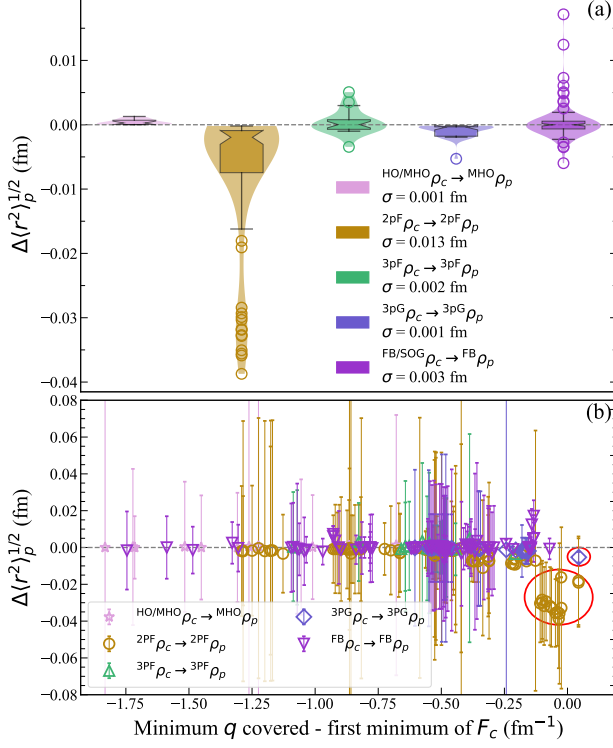


FIG. 4: (a) Violin and box plots on the radius differences $\Delta\langle r^2 \rangle_p^{1/2}$. The different density distributions are distinguished. The root mean square deviations are also given. See the text for more details. (b) The radius differences $\Delta\langle r^2 \rangle_p^{1/2}$ as a function of the minimum q covered in the experiments minus the first minimum of F_c . The circled data corresponds to the outliers of 2pF and 3pG in Fig. 4 (a). Data listed in Tab. I are excluded.

(Q3), respectively. The area between Q1 and Q3 is the interquartile range, $IQR = Q3 - Q1$. The groove inside the box indicates the median value. The T-shaped whiskers extend to the furthest data points within 1.5 times the interquartile range from Q1 to Q3. Data outside this range are considered extreme values (outliers) and plotted as empty circles. The violin plots display the data density at different values, reflecting the overall distribution shape and making it easier to visualize the concentration and distribution characteristics of the data. Taking 2pF data (the second box in Fig. 4 (a)) as an example, the median value of the data set is approximately 0.002 fm. Two whiskers encompass data agrees within 0.018 fm. Outliers outside the lower whisker are identified by hollow circles with 0.018 to 0.04 fm deviations.

It is observed that MHO achieves an accuracy of 0.002 fm, demonstrating its reliability

and applicability in describing the density distribution of nuclei with $Z \leq 8$. For heavier nuclei, the most commonly applied 2pF function achieves radius accuracy within 0.002 fm except for the marked outliers. With an additional inner depth parameter in Eqs. (12) and (13), 3pF and 3pG data exhibit significantly narrower and more compact deviation distributions, reaching the level of 0.004 fm. They also have fewer outliers recognized than the 2pF case.

The first dip of the form factor needs to be covered in experiments to determine the radius information [13]. As depicted in Fig. 2 (a) and (d), the relatively low q region, sensitive to the surface area, is crucial for determining rms radii. The deviations of rms radii are illustrated as a function of the minimum q (q_{\min}) reached in experiments, minus the first minimum of F_c in Fig. 4 (b). The radius deviations $\Delta\langle r^2 \rangle_p^{1/2}$ increases considerably when q_{\min} is close to the first minimum of F_c . For 2pF cases, the deviations reach 0.04 fm, while around 0.005 fm for 3pG. These outliers in the box plots in Fig. 4 (a) are also marked with red circles in Fig. 4 (b) and enumerated in Tab. II. Most of data predominantly come from the same study [30] with relatively higher q_{\min} (close to 1 fm^{-1}). Most of these data have deviations outside the experimental uncertainties. These data also deviate from others and should be used with caution. Taking ^{54}Cr as an example, it gives $\langle r^2 \rangle_c^{1/2} 3.776(15)$ fm, while the other two results give 3.673(14) and 3.689(4) fm for which both q_{\min} values 0.15 fm^{-1} . As for the three outliers marked in 3pF cases, no pronounced correlation is observed. These anomalies could be due to experimental errors or inherent biases since they are measured with a suitable q_{range} .

In this work, F_c obtained from ρ_c is considered as experimental data to deduce ρ_p , which has the same q_{range} as the experiment covered. The point-proton density ρ_p with predefined distribution functions cannot fully capture F_c shape within experiment q_{range} . At the same time, F_c information beyond q_{range} is lacking. The two reasons above lead to the radii discrepancies between ${}^1\langle r^2 \rangle_p^{1/2}$ and ${}^2\langle r^2 \rangle_p^{1/2}$. We conclude that if q_{\min} is far below the first dip of F_c , the accuracy is overall 0.01 fm for 2pF, 0.002 fm for MHO (for $Z \leq 8$ nuclei) and 0.004 fm for 3pF, and 3pG. If one aims for a radius precision of 0.01 fm in the experiment, 2pF with an adequate q_{range} is sufficient.

TABLE II: Outliers of 2pF, 3pG and FB marked in Fig. 4 (a). The model of ρ_c , minimum q reached in experiments, and the radius difference $\Delta\langle r^2 \rangle_p^{1/2}$ are listed in the second, third, and fourth columns, respectively.

Nucleus	Model	Minimum q (fm $^{-1}$)	$\Delta\langle r^2 \rangle_p^{1/2}$ (fm)
^{50}Cr	2pF	0.97	-0.030(17)
^{52}Cr	2pF	0.97	-0.028(17)
^{53}Cr	2pF	0.97	-0.030(17)
^{54}Cr	2pF	0.97	-0.032(17)
^{54}Fe	2pF	0.97	-0.029(18)
^{56}Fe	2pF	0.97	-0.032(17)
^{58}Fe	2pF	1.02	-0.039(22)
^{59}Co	2pF	0.96	-0.033(21)
^{63}Cu	2pF	0.96	-0.036(17)
^{65}Cu	2pF	0.96	-0.035(17)
^{66}Zn	2pF	0.96	-0.036(35)
^{68}Zn	2pF	0.96	-0.033(41)
^{118}Sn	2pF	0.84	-0.019(24)
^{124}Sn	2pF	0.84	-0.018(24)
^{209}Bi	3pG	0.70	-0.005(31)
^{16}O	FB	0.29	0.003(11)
^{50}Cr	FB	0.15	0.006(5)
^{52}Cr	FB	0.15	0.007(4)
^{54}Cr	FB	0.15	0.004(5)
^{64}Ni	FB	0.51	-0.006(34)
^{66}Zn	FB	0.51	-0.003(36)
^{98}Mo	FB	0.56	-0.003(22)
^{144}Sm	FB	0.60	0.005(12)
^{148}Sm	FB	0.60	0.005(8)
^{150}Sm	FB	0.60	0.012(8)
^{152}Sm	FB	0.60	0.017(8)
^{166}Er	FB	0.29	-0.003(28)
^{174}Yb	FB	0.32	0.004(42)

The outliers in FB cases in Fig. 4(a) are listed in Tab. II. Overall, most of the outliers fall within the error bars, and they exhibit no obvious correlation with q_{\min} , as demonstrated in

Fig. 4 (b). We take ^{50}Ti and ^{50}Cr as examples. Their radius differences are -0.002(3) and 0.006(6) fm (see Tab IV in Appendix for details). Their deduced F_p , and the relevant densities ρ_p are compared in Fig. 5. Two F_p start to deviate considerably from each other when q exceeds 3 fm $^{-1}$, reflecting the uncertainties caused by extrapolation beyond experimental q_{range} . The differences at high q are accordingly reflected in the central density distributions. As shown by the inset, a significant difference between the two density distributions in the center region is observed. Therefore, caution should be taken when utilizing the central density pattern and form factor at high q for the few data with large $\Delta\langle r^2 \rangle_p^{1/2}$ values.

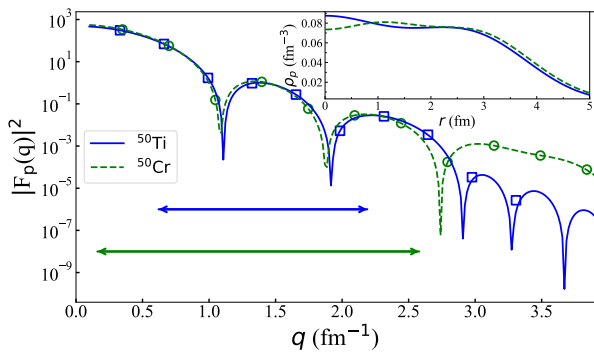


FIG. 5: The deduced F_p of ^{50}Ti and ^{50}Cr in the FB form with blue solid and green dashed lines respectively. The points are FB coefficients. Arrows represent q_{range} covered in experiments. The inset is the corresponding ρ_p .

B. Two-parameter Fermi point-proton densities

For nuclei with $Z > 8$, most of the data have been given in the 2pF distribution [10]:

$$\rho(r) = \frac{\rho_0}{1 + e^{\frac{r-c}{z}}}, \quad (7)$$

where ρ_0 , c , and z are the normalization coefficient, half-density radius, and surface diffuseness, respectively. This allows a systematic comparison of the density shapes and parameters between ρ_c and ρ_p . Taking ^{116}Sn as an example, its ρ_p and ρ_c are shown in Fig. 6. Although having similar distributions, the surface diffuseness parameter z decreases slightly from 0.550(9) fm in ρ_c to 0.502(5) fm in ρ_p , while the radius parameter c remains almost unchanged, merely varying from 5.358(22) to 5.377(21) fm.

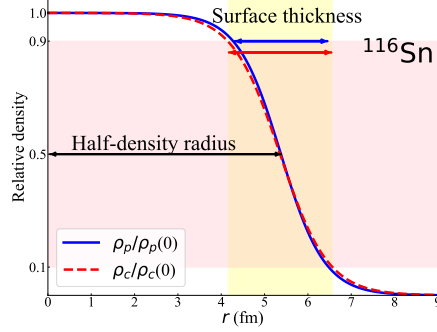


FIG. 6: Charge density ρ_c (red dashed line) and point-proton density ρ_p (blue solid line) of ^{116}Sn in the 2pF form. The density is scaled by dividing the central density $\rho(0)$. The half-density radius and surface thickness are also indicated.

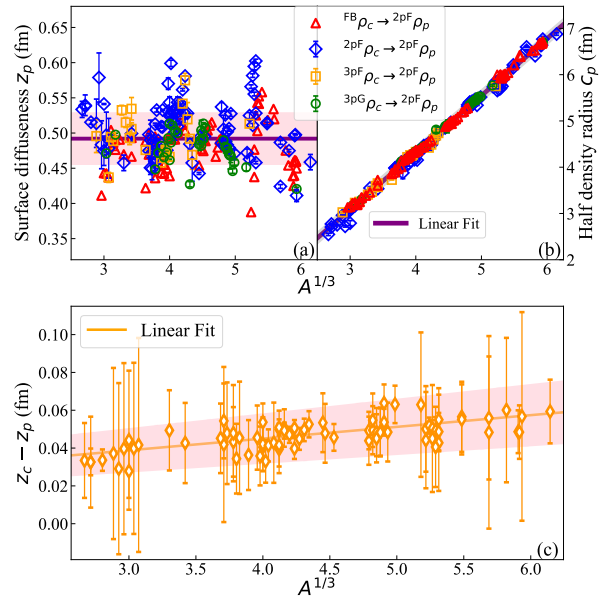


FIG. 7: (a) Surface diffuseness z_p and (b) half-density radius c_p of point-proton density ρ_p in 2pF form from four kinds of ρ_c as a function of $A^{1/3}$. The solid line in (a) is the average value and the colored region represents the standard deviation. (c) Difference in surface diffuseness parameters between ρ_c and ρ_p , $z_c - z_p$, as a function of $A^{1/3}$. The solid line illustrates the linear fit of $z_c - z_p$. The colored region depicts the loci of the regression's 95% confidence bands.

The deduced ρ_p parameters in 2pF form from ρ_c in 2pF, 3pF, 3pG and FB forms, are presented in Fig. 7 (a) and (b). Data listed in Tabs. I and II are excluded. The surface parameters (z_p) exhibit an average value of 0.49 fm with a standard deviation of 0.037 fm. It is also evident that some 2pF data exhibit significant biases. Even for the same

nuclei, surface parameters can significantly differ in different experimental results due to different q_{range} . This is also noticed in muonic atom spectroscopy [31]. For example, two existing measurements for ^{146}Nd mainly differing in maximum q reached, namely, 0.73 and 2.94 fm^{-1} , have the surface parameters of $0.6321(30) \text{ fm}$ and $0.556(20) \text{ fm}$, while the radius parameters of 5.6541 fm and $5.867(32) \text{ fm}$. However, they give consistent rms radii, namely, $4.970(5) \text{ fm}$ and $4.993(37) \text{ fm}$.

In Fig. 7 (b), the deduced half-density radius parameters (c_p) of 2pF ρ_p , derived from 2pF, 3pF, 3pG, and FB ρ_c , all exhibit a clear adherence to the $A^{1/3}$ rule, namely,

$$c_p = 1.232(6)A^{1/3} - 0.612(25). \quad (8)$$

The linear coefficient of 0.995 indicates the consistency among different types of ρ_c data.

Figure 7 (c) presents the difference between ρ_c and ρ_p surface diffuseness parameters as a function of $A^{1/3}$. The difference is much larger than the experiment uncertainties (typically 0.019 fm). The difference increases smoothly with c_c , indicating the contribution of single-proton charge density is more significant as nuclei become heavier. The following empirical formula can describe the systemic difference in surface parameters:

$$z_p = z_c - (0.0062(8)A^{1/3} + 0.020(4)). \quad (9)$$

Although the linear coefficient of 0.5 indicates a moderate correlation, this relationship still captures the general variation trend of the diffuseness parameters. A moderate correlation may arise from inconsistencies in surface parameters across the results of different experiments. Eqs. (9) and (8) offer an empirical way to determine ρ_p from ρ_c in 2pF case, and vice versa. The formulas will be useful for a quick estimation of ρ_p .

C. Point-proton densities for ^{48}Ca and ^{208}Pb

Neutron skin thickness of ^{48}Ca and ^{208}Pb serve as ideal targets for investigating the equation of state of nuclear matter. Their relevant point-proton density distributions are fundamentally important as inputs for the analysis of neutron density distribution and neutron-skin thickness.

There are three experimental ρ_c results for ^{48}Ca , which are presented in the 3pF, FB, and SOG forms, respectively. Their corresponding ${}^1\langle r^2 \rangle_p^{1/2}$ are 3.388 , $3.370(9)$ and 3.379 fm . ρ_p

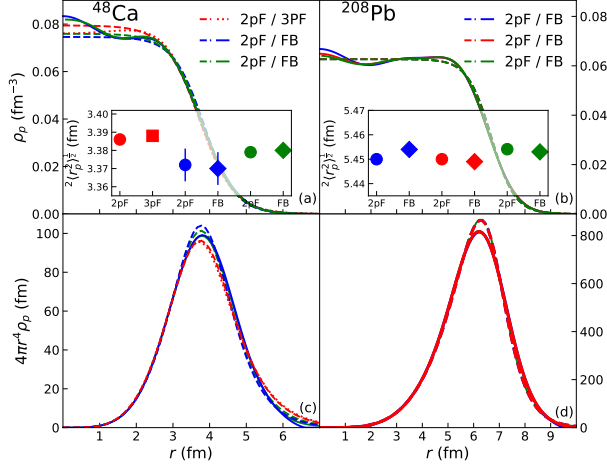


FIG. 8: The deduced ρ_p of ^{48}Ca (a) and ^{208}Pb (b) and their relevant radial integrated (c) and (d) in the FB form (solid line), the 2pF form (dashed line), and the 3pF form (dotted line). The inset is the corresponding ${}^2\langle r^2 \rangle_p^{1/2}$ with 2pF, 3pF, and FB in circle, square, and diamond, respectively.

in two different density forms can be deduced for each ρ_c form. For example, for ρ_c in the FB form, we have given ρ_p in 2PF and FB forms. For ^{208}Pb , there are three experimental ρ_c results, two of which are in the FB forms and the other in the SOG form. They give ${}^1\langle r^2 \rangle_p^{1/2}$ of 5.454(2), 5.450(1) and 5.454(2) fm, respectively. In total, six different ρ_p and ${}^2\langle r^2 \rangle_p^{1/2}$ are presented for both ^{48}Ca and ^{208}Pb . The details can be found in Tables. III and IV.

In Fig. 8 (a) and (b), we present the deduced ρ_p in various density forms for ^{48}Ca and ^{208}Pb . Similar to the case in Fig. 2, the 2pF, 3pF and FB cases exhibit similar behavior at the tail, while more details are provided in FB form at the central range than a completely flat distribution given by 2pF. The 2pF, 3pF, and FB cases provide almost identical ${}^2\langle r^2 \rangle_p^{1/2}$, indicating the consistency of different density distributions in describing radii. The radial integrand functions are presented in Fig. 8 (c) and (d). The interior oscillations in the volume integral are negligible, while the most significant differences occur at the maximum value of the radial integral. In all, the 2pF and 3pF ρ_p provide sufficient precision for the radius, but FB offers more detailed density.

IV. SUMMARY

In this paper, we deduce the point-proton density distributions of 130 stable nuclei from ^7Li to ^{232}Th by unfolding ρ_c measured in elastic electron scattering. The $\langle r^2 \rangle_p^{1/2}$ values

calculated from the derived ρ_p agree in 0.2% with the one directly obtained from $\langle r^2 \rangle_c^{1/2}$ in model-dependent forms. This is smaller than the experimental radius accuracy. We have identified cases exhibiting large $\langle r^2 \rangle_p^{1/2}$ deviations due to the limited q coverage in experiments or inconsistent scattering experiments. Caution is advised when using these data. In the 2pF cases, the surface diffuseness parameter of ρ_p shows a reduction of about 10% compared to that of ρ_c . The transition from ρ_c to ρ_p for the surface parameter follows a linear trend with $A^{1/3}$, whereas the half-density radius parameter remains almost unchanged and follows well the $A^{1/3}$ rule. Finally, we show the ρ_p for ^{48}Ca and ^{208}Pb , the two important nuclei for studying nuclear equation of state. The derived point-proton densities can be used as inputs for nuclear reaction models and assessments of nuclear structure models. Moreover, they can be benchmarks when extracting radii in charge-changing cross-section measurements of unstable nuclei and a basis for analyzing experimental data to extract neutron skin.

Acknowledgments

Discussions with S. Terashima and J. Li are gratefully acknowledged. This work was partly supported by the National Natural Science Foundation of China (Nos. 12325506, 11961141004, 11922501, 12475119) and the 111 Center (Grant No. B20065).

Model-dependent and model-independent densities distribution

The nuclear charge density distributions are usually written in parameterized functions, including HO, MHO, 2pF, 3pF, 3pG, SOG, and FB.

The model-dependent Harmonic-oscillator function is written as [10]:

$$\rho(r) = \rho_0(1 + \alpha(\frac{r}{a})^2)e^{-(\frac{r}{a})^2}, \quad (10)$$

where $\alpha = \frac{\alpha_0 a_0^2}{a^2 + \frac{3}{2}\alpha_0(a^2 - a_0^2)}$, $a_0^2 = \frac{A(a^2 - a_p^2)}{A-1}$, $\alpha_0 = \frac{Z-2}{3}$, $a_p^2 = \frac{2}{3}r_p^2$. The modified harmonic-oscillator model has the same expression as HO but with α as an additional free parameter.

The model-dependent two-parameter Fermi function is written as:

$$\rho(r) = \rho_0 \frac{1}{1 + e^{\frac{r-c}{z}}}, \quad (11)$$

where c and z correspond to the half-density and the surface diffuseness parameter, respectively.

The model-dependent three-parameter Fermi function is written as:

$$\rho(r) = \rho_0 \frac{1 + w \frac{r^2}{c^2}}{1 + e^{\frac{r-c}{z}}}, \quad (12)$$

where w corresponds to the inner depth parameter.

The model-dependent three-parameter Gaussian function is described as:

$$\rho(r) = \rho_0 \frac{1 + w \frac{r^2}{c^2}}{1 + e^{\frac{r^2 - c^2}{z^2}}}. \quad (13)$$

The model-independent Fourier-Bessel series [15]:

$$\rho(r) = \begin{cases} \sum_{\nu}^{N_{FB}} a_{\nu} j_0\left(\frac{\nu \pi r}{R_{cut}}\right), & \text{for } r \leq R_{cut}, \\ 0 & \text{for } r > R_{cut}, \end{cases} \quad (14)$$

where $j_0\left(\frac{\nu \pi r}{R_{cut}}\right) = \frac{\sin(\nu \pi r / R_{cut})}{\nu \pi r / R_{cut}}$ denotes the Bessel function of order zero, and R_{cut} is the cutoff radius of the charge distribution, truncating the expansion after ν terms and assuming the charge is zero for $r \geq R_{cut}$. The coefficients a_{ν} can be determined by the F_c ,

$$a_{\nu} = \frac{q_{\nu}^2}{2\pi R_{cut}} F_c(q_{\nu}) \quad \text{with} \quad q_{\nu} = \frac{\nu \pi}{R_{cut}}. \quad (15)$$

The considered number of FB coefficients is related to the maximum value of the momentum transfer q_{\max} :

$$N_{\text{FB}} = \frac{R_{\text{cut}} q_{\max}}{\pi}. \quad (16)$$

The model-independent Sum-of-Gaussians function:

$$\rho(r) = \frac{Z}{2\pi^{\frac{3}{2}}\gamma^3} \sum_{i=1}^{12} \frac{Q_i}{1 + \frac{2R_i^2}{\gamma^2}} [e^{-(\frac{r-R_i}{\gamma})^2} + e^{-(\frac{r+R_i}{\gamma})^2}], \quad (17)$$

where R_i and Q_i are the position and amplitude of the Gaussians. The value of Q_i indicates the fraction of charge contained in the i^{th} Gaussian, normalized such that $\sum_i Q_i = 1$, and γ is the rms radius of the Gaussians.

Explanation of Tables

Table III. Point-proton density distribution parameters

ρ_c	Density distribution function for ρ_c
$\langle r^2 \rangle_c^{1/2}$	rms charge radius
${}^1\langle r^2 \rangle_p^{1/2}$	rms point-proton radius calculated from $\langle r^2 \rangle_c^{1/2}$
ρ_p	Density distribution function adopted for the deduced ρ_p
${}^2\langle r^2 \rangle_p^{1/2}$	rms point-proton radius calculated from the deduced ρ_p
c or a	The values are given for the parameter c if 2PF, 3PF, or 3PG model has been used and for the parameter a if the MHO model has been used
z or α	The values are given for the parameter z if 2PF, 3PF, or 3PG model has been used and for the parameter α if the MHO model has been used
w	The parameter w of the 3PF and 3PG models
$\Delta\langle r^2 \rangle_p^{1/2}$	${}^2\langle r^2 \rangle_p^{1/2} - {}^1\langle r^2 \rangle_p^{1/2}$
HO	Harmonic-oscillator model
MHO	Modified harmonic-oscillator model
2pF	Two-parameter Fermi model
3pF	Three-parameter Fermi model
3pG	Three-parameter Gaussian model
FB	Fourier-Bessel expansion

TABLE III: Point-proton density distribution parameters.
Units are fm.

Nucleus	ρ_c	$\langle r^2 \rangle_c^{1/2}$ (fm)	${}^1\langle r^2 \rangle_p^{1/2}$ (fm)	ρ_p	${}^2\langle r^2 \rangle_p^{1/2}$ (fm)	c or a (fm)	z or α (fm)	w	$\Delta\langle r^2 \rangle_p^{1/2}$ (fm)
${}^7\text{Li}$	HO	2.394(30)	2.274(30)	MHO	2.274(30)	1.656(16)	0.419(45)		0.00(4)
${}^9\text{Be}$	HO	2.519(13)	2.403(13)	MHO	2.403(14)	1.676(16)	0.832(45)		0.00(1)
${}^9\text{Be}$	HO	2.495(100)	2.377(100)	MHO	2.377(101)	1.653(16)	0.874(45)		0.00(14)
${}^{10}\text{B}$	HO	2.452(140)	2.327(140)	MHO	2.328(143)	1.586(16)	1.261(45)		0.001(200)
${}^{11}\text{B}$	HO	2.419(140)	2.297(140)	MHO	2.297(143)	1.570(16)	1.199(45)		0.001(200)
${}^{12}\text{C}$	FB	2.478(15)	2.348(15)	MHO	2.354(15)	1.605	1.164		0.007(21)
				FB	2.346(15)				-0.002(21)
${}^{12}\text{C}$	FB	2.464(12)	2.339(12)	MHO	2.339(12)	1.594	1.230		-0.000(17)
				FB	2.339(12)				0.000(17)
${}^{12}\text{C}$	FB	2.485(9)	2.354(9)	MHO	2.361(9)	1.589	1.399		0.007(13)
				FB	2.353(9)				-0.001(13)
${}^{12}\text{C}$	SOG	2.469(6)	2.345(6)	2pF	2.346(6)	2.265	0.419		0.001(8)
				FB	2.346(6)				0.001(8)
${}^{13}\text{C}$	MHO	2.413(10)	2.290(10)	MHO	2.290(14)	1.509(16)	2.694(45)		0.00(1)
${}^{14}\text{C}$	MHO	2.551(60)	2.438(60)	MHO	2.440(62)	1.619(16)	2.253(45)		0.001(86)
${}^{14}\text{N}^3$	HO	2.58	2.462	MHO	2.463	1.642	1.999		0.001
${}^{14}\text{N}$	HO	2.541(20)	2.420(20)	MHO	2.420(22)	1.604(16)	2.333(45)		0.00(3)
${}^{15}\text{N}^3$	MHO	2.655	2.543	MHO	2.544	1.699	1.930		0.001
${}^{15}\text{N}$	FB	2.611(8)	2.497(8)	MHO	2.354(8)	1.750	0.713		0.009(11)
				FB	2.496(8)				-0.001(11)
${}^{15}\text{N}$	FB	2.613(5)	2.499(5)	MHO	2.339(5)	1.745	0.740		0.003(8)
				FB	2.499(5)				0.000(8)
${}^{16}\text{O}$	HO	2.718(21)	2.605(21)	MHO	2.606(22)	1.716(16)	2.747(45)		0.00(3)
${}^{16}\text{O}$	FB	2.737(9)	2.625(9)	MHO	2.361(9)	1.797	1.064		0.016(13)
				FB	2.628(9)				0.003(13)

(continued)

TABLE III – (*continued*)

Nucleus	ρ_c	$\langle r^2 \rangle_c^{1/2}$ (fm)	${}^1\langle r^2 \rangle_p^{1/2}$ (fm)	ρ_p	${}^2\langle r^2 \rangle_p^{1/2}$ (fm)	c or a (fm)	z or α (fm)	w	$\Delta\langle r^2 \rangle_p^{1/2}$ (fm)
${}^{16}\text{O}^{\textcolor{blue}{3}}$	SOG	2.711	2.598	2pF FB	2.598 2.597	2.592	0.443		0.000 -0.001
${}^{17}\text{O}$	HO	2.662(28)	2.550(28)	MHO	2.550(29)	1.684(16)	2.576(45)		0.00(4)
${}^{18}\text{O}$	HO	2.727(21)	2.620(21)	MHO	2.621(22)	1.733(16)	2.472(45)		0.00(3)
${}^{19}\text{F}$	2pF	2.904(42)	2.801(42)	2pF	2.798(31)	2.549(26)	0.534(11)		-0.003(52)
${}^{20}\text{Ne}$	2pF	3.037(15)	2.937(15)	2pF	2.935(10)	2.773(9)	0.538(3)		-0.002(18)
${}^{20}\text{Ne}$	2pF	3.004(50)	2.903(50)	2pF	2.901(39)	2.706(29)	0.539(14)		-0.002(63)
${}^{20}\text{Ne}^{\textcolor{blue}{1}}$	3pF	2.949(33)	2.845(33)	2pF 3pF	2.879(36) 2.849(33)	2.847(15) 2.795(4)	0.498(15) 0.657(2)	-0.187(10)	0.034(49) 0.004(47)
${}^{22}\text{Ne}$	2pF	2.968(12)	2.869(12)	2pF	2.867(8)	2.754(8)	0.515(2)		-0.002(14)
${}^{24}\text{Mg}$	3pF	3.071(65)	2.972(65)	2pF 3pF	2.981(51) 2.975(94)	3.025(19) 3.115(18)	0.496(23) 0.536(4)	-0.151(68)	0.009(83) 0.003(83)
${}^{24}\text{Mg}^{\textcolor{blue}{1}}$	3pF	2.956(58)	2.853(58)	2pF 3pF	2.889(41) 2.864(60)	3.066(19) 3.249(11)	0.443(19) 0.529(5)	-0.289(33)	0.036(71) 0.011(83)
${}^{24}\text{Mg}$	2pF	3.086(82)	2.987(82)	2pF	2.986(78)	2.962(23)	0.514(34)		-0.001(113)
${}^{24}\text{Mg}^{\textcolor{blue}{3}}$	SOG	3.027	2.927	2pF FB	2.936 2.927	3.024	0.476		0.009 0.000
${}^{25}\text{Mg}$	2pF	3.111(87)	3.014(87)	2pF	3.012(88)	2.722(16)	0.579(34)		-0.002(124)
${}^{25}\text{Mg}^{\textcolor{blue}{1}}$	3pF	2.982(104)	2.882(104)	2pF 3pF	2.890(114) 2.883(138)	3.143(14) 3.269(11)	0.419(57) 0.522(10)	-0.284(77)	0.008(154) 0.001(173)
${}^{26}\text{Mg}$	2pF	3.060(80)	2.963(80)	2pF	2.962(75)	3.039(26)	0.483(34)		-0.001(110)
${}^{26}\text{Mg}$	FB	2.961(4)	2.862(4)	2pF FB	2.867(4) 2.862(4)	3.132	0.411		0.002(6) 0.000(6)
${}^{27}\text{Al}$	2pF	3.062(87)	2.964(87)	2pF	2.961(70)	3.069(74)	0.475(20)		-0.003(112)
${}^{27}\text{Al}$	2pF	3.051(38)	2.953(38)	2pF	2.953(33)	2.791(54)	0.541(0)		0.00(5)

(continued)

TABLE III – (*continued*)

Nucleus	ρ_c	$\langle r^2 \rangle_c^{1/2}$ (fm)	${}^1\langle r^2 \rangle_p^{1/2}$ (fm)	ρ_p	${}^2\langle r^2 \rangle_p^{1/2}$ (fm)	c or a (fm)	z or α (fm)	w	$\Delta\langle r^2 \rangle_p^{1/2}$ (fm)
${}^{27}\text{Al}$	FB	3.035(2)	2.937(2)	2pF	2.939(2)	3.143	0.443		0.001(3)
				FB	2.936(2)				-0.001(3)
${}^{28}\text{Si}$	3pG	3.107(12)	3.009(12)	2pF	3.018(9)	3.174(13)	0.471(1)		0.009(15)
				3pG	3.009(10)	2.144(15)	1.955(8)	0.458(0)	0.000(16)
${}^{28}\text{Si}$	2pF	3.146(84)	3.050(84)	2pF	3.048(74)	3.130(36)	0.497(32)		-0.002(112)
${}^{28}\text{Si}^{\textcolor{blue}{1}}$	3pF	3.076(18)	2.977(18)	2pF	2.983(15)	3.244(2)	0.433(8)		0.006(23)
				3pF	2.977(21)	3.387(0)	0.520(2)	-0.278(14)	0.000(28)
${}^{28}\text{Si}$	FB	3.085(17)	2.986(17)	2pF	2.989(17)	3.221	0.443		-0.005(24)
				FB	2.986(17)				0.000(24)
${}^{28}\text{Si}^{\textcolor{blue}{3}}$	SOG	3.153	3.056	2pF	3.059	3.185	0.487		0.003
				FB	3.057				0.001
${}^{29}\text{Si}$	2pF	3.125(108)	3.029(108)	2pF	3.027(99)	3.163(54)	0.478(42)		-0.002(147)
${}^{29}\text{Si}$	3pF	3.078(19)	2.980(19)	2pF	2.983(14)	3.230(8)	0.437(7)		0.003(24)
				3pF	2.981(28)	3.362(7)	0.477(2)	-0.217(27)	0.001(24)
${}^{29}\text{Si}$	FB	3.080(17)	2.983(17)	2pF	2.984(17)	3.231	0.437		-0.006(24)
				FB	2.983(17)				0.000(24)
${}^{30}\text{Si}$	3pF	3.178(28)	3.085(28)	2pF	3.085(20)	3.198(20)	0.494(7)		0.000(34)
				3pF	3.085(42)	3.124(21)	0.482(1)	0.126(70)	0.000(34)
${}^{30}\text{Si}$	FB	3.173(25)	3.080(25)	2pF	3.079(25)	3.201	0.491		0.003(36)
				FB	3.080(25)				0.000(36)
${}^{30}\text{Si}^{\textcolor{blue}{2}}$	FB	3.193(13)	3.101(13)	2pF	3.098(13)	3.185	0.504		0.003(19)
				FB	3.099(13)				-0.002(19)
${}^{31}\text{P}$	3pF	3.192(42)	3.099(42)	2pF	3.107(28)	3.254(25)	0.489(11)		0.008(50)
				3pF	3.102(45)	3.335(11)	0.502(3)	-0.110(48)	0.003(50)
${}^{31}\text{P}$	FB	3.187(10)	3.093(10)	2pF	3.093(10)	3.257	0.482		0.001(14)
				FB	3.092(10)				-0.001(14)
${}^{31}\text{P}$	FB	3.191(5)	3.097(5)	2pF	3.098(5)	3.248	0.486		-0.001(7)
				FB	3.096(5)				-0.001(7)
${}^{32}\text{S}$	3pG	3.239(20)	3.145(20)	2pF	3.158(26)	3.304(39)	0.498(2)		0.013(33)
				3pG	3.145(15)	2.651(65)	2.061(3)	0.254(12)	0.000(25)

(continued)

TABLE III – (*continued*)

Nucleus	ρ_c	$\langle r^2 \rangle_c^{1/2}$ (fm)	${}^1\langle r^2 \rangle_p^{1/2}$ (fm)	ρ_p	${}^2\langle r^2 \rangle_p^{1/2}$ (fm)	c or a (fm)	z or α (fm)	w	$\Delta\langle r^2 \rangle_p^{1/2}$ (fm)
${}^{32}\text{S}$	FB	3.248(4)	3.155(4)	2pF	3.160(4)	3.334	0.490		0.000(6)
				FB	3.155(4)				0.000(6)
${}^{32}\text{S}^{\textcolor{blue}{2}}$	FB	3.228(5)	3.134(5)	2pF	3.140(5)	3.347	0.476		0.006(7)
				FB	3.132(5)				-0.002(7)
${}^{32}\text{S}^{\textcolor{blue}{3}}$	SOG	3.258	3.165	2pF	3.161	3.291	0.503		-0.004
				FB	3.163				-0.002
${}^{34}\text{S}$	FB	3.281(4)	3.190(4)	2pF	3.195(4)	3.387	0.491		0.005(6)
				FB	3.190(4)				0.000(6)
${}^{36}\text{S}$	FB	3.278(6)	3.190(6)	2pF	3.195(6)	3.455	0.470		0.006(9)
				FB	3.189(6)				-0.001(9)
${}^{35}\text{Cl}$	3pF	3.388(35)	3.300(35)	2pF	3.299(25)	3.408(31)	0.533(6)		-0.001(43)
				3pF	3.300(27)	3.387(7)	0.529(3)	0.028(35)	0.000(43)
${}^{37}\text{Cl}$	3pF	3.383(33)	3.297(33)	2pF	3.298(23)	3.467(27)	0.515(7)		0.001(40)
				3pF	3.298(28)	3.487(2)	0.518(3)	-0.027(36)	0.001(40)
${}^{36}\text{Ar}$	2pF	3.327(41)	3.236(41)	2pF	3.233(32)	3.550(32)	0.458(11)		-0.003(52)
${}^{40}\text{Ar}$	3pF	3.471(78)	3.388(78)	2pF	3.405(52)	3.571(58)	0.534(15)		0.017(94)
				3pF	3.393(69)	3.696(6)	0.546(6)	-0.138(64)	0.005(94)
${}^{40}\text{Ar}$	2pF	3.396(42)	3.311(42)	2pF	3.308(31)	3.535(31)	0.499(11)		-0.003(52)
${}^{40}\text{Ar}$	FB	3.424(14)	3.339(14)	2pF	3.340(14)	3.604	0.493		0.001(20)
				FB	3.339(14)				0.000(20)
${}^{39}\text{K}$	3pF	3.414(37)	3.326(37)	2pF	3.333(26)	3.595(26)	0.493(9)		0.007(45)
				3pF	3.328(37)	3.717(6)	0.508(3)	-0.154(40)	0.002(45)
${}^{39}\text{K}^{\textcolor{blue}{3}}$	SOG	3.427	3.340	2pF	3.343	3.588	0.500		0.003
				FB	3.341				0.001
${}^{40}\text{Ca}$	3pF	3.481(34)	3.394(34)	2pF	3.397(24)	3.652(25)	0.506(8)		0.003(42)
				3pF	3.395(35)	3.714(7)	0.514(3)	-0.083(42)	0.001(42)
${}^{40}\text{Ca}$	FB	3.450(10)	3.362(10)	2pF	3.365(10)	3.722	0.467		0.002(14)
				FB	3.362(10)				0.000(14)
${}^{40}\text{Ca}$	SOG	3.48(3)	3.393(3)	2pF	3.388(3)	3.651	0.502		-0.005(4)
				FB	3.394(3)				0.001(4)

(continued)

TABLE III – (*continued*)

Nucleus	ρ_c	$\langle r^2 \rangle_c^{1/2}$ (fm)	${}^1\langle r^2 \rangle_p^{1/2}$ (fm)	ρ_p	${}^2\langle r^2 \rangle_p^{1/2}$ (fm)	c or a (fm)	z or α (fm)	w	$\Delta\langle r^2 \rangle_p^{1/2}$ (fm)
${}^{48}\text{Ca}^3$	3pF	3.469	3.388	2pF	3.386	3.727	0.476	0.153	-0.002
				3pF	3.388	3.626	0.472		0.000
${}^{48}\text{Ca}$	FB	3.451(9)	3.370(9)	2pF	3.372(9)	3.854	0.422		0.002(13)
				FB	3.370(9)				0.000(13)
${}^{48}\text{Ca}^3$	SOG	3.46	3.379	2pF	3.380	3.814	0.442		0.001
				FB	3.380				0.001
${}^{48}\text{Ti}^1$	2pF	3.693(14)	3.614(14)	2pF	3.576(9)	3.879(13)	0.522(1)		-0.038(17)
${}^{48}\text{Ti}$	FB	3.597(1)	3.516(1)	2pF	3.505(1)	3.872	0.488		-0.011(1)
				FB	3.515(1)				-0.001(1)
${}^{50}\text{Ti}^2$	FB	3.572(2)	3.492(2)	2pF	3.483(2)	3.891	0.469		-0.009(3)
				FB	3.490(2)				-0.002(3)
${}^{51}\text{V}$	2pF	3.583(34)	3.502(34)	2pF	3.498(26)	3.964(26)	0.451(9)		-0.004(43)
${}^{51}\text{V}$	2pF	3.617(64)	3.537(64)	2pF	3.536(56)	3.912(26)	0.490(28)		-0.001(85)
${}^{50}\text{Cr}$	2pF	3.638(33)	3.556(33)	2pF	3.555(25)	3.984(23)	0.475(10)		-0.001(41)
${}^{50}\text{Cr}^2$	2pF	3.707(14)	3.627(14)	2pF	3.597(10)	3.982(13)	0.498(1)		-0.030(17)
${}^{50}\text{Cr}^2$	FB	3.663(4)	3.581(4)	2pF	3.577(4)	3.950	0.498		-0.004(6)
				FB	3.587(4)				0.006(6)
${}^{52}\text{Cr}$	2pF	3.614(46)	3.533(46)	2pF	3.532(37)	4.018(32)	0.449(15)		-0.001(59)
${}^{52}\text{Cr}^2$	2pF	3.685(14)	3.606(14)	2pF	3.577(10)	4.024(14)	0.472(1)		-0.029(17)
${}^{52}\text{Cr}^2$	FB	3.644(3)	3.563(3)	2pF	3.557(3)	3.964	0.483		-0.006(4)
				FB	3.570(3)				0.007(4)
${}^{53}\text{Cr}^2$	2pF	3.726(14)	3.649(14)	2pF	3.619(10)	4.039(13)	0.489(1)		-0.030(17)
${}^{54}\text{Cr}$	2pF	3.674(33)	3.595(33)	2pF	3.594(25)	4.026(24)	0.481(9)		-0.001(41)
${}^{54}\text{Cr}^2$	2pF	3.777(14)	3.701(14)	2pF	3.669(10)	4.047(13)	0.513(1)		-0.032(17)
${}^{54}\text{Cr}^2$	FB	3.689(4)	3.611(4)	2pF	3.607(4)	4.006	0.495		-0.003(6)
				FB	3.615(4)				0.004(6)

(continued)

TABLE III – (*continued*)

Nucleus	ρ_c	$\langle r^2 \rangle_c^{1/2}$ (fm)	${}^1\langle r^2 \rangle_p^{1/2}$ (fm)	ρ_p	${}^2\langle r^2 \rangle_p^{1/2}$ (fm)	c or a (fm)	z or α (fm)	w	$\Delta\langle r^2 \rangle_p^{1/2}$ (fm)
${}^{55}\text{Mn}$	2pF	3.677(90)	3.598(90)	2pF	3.598(91)	3.878(126)	0.533(2)		0.00(12)
${}^{54}\text{Fe}$	3pG	3.683(14)	3.602(14)	2pF	3.603(11)	4.124(15)	0.448(2)		0.001(18)
				3pG	3.601(12)	3.603(9)	2.138(10)	0.510(27)	-0.001(18)
${}^{54}\text{Fe}$	2pF	3.674(44)	3.593(44)	2pF	3.592(34)	4.084(30)	0.458(14)		-0.001(56)
${}^{54}\text{Fe}^2$	2pF	3.732(15)	3.652(15)	2pF	3.623(10)	4.112(12)	0.464(1)		-0.029(18)
${}^{54}\text{Fe}$	FB	3.663(25)	3.582(25)	2pF	3.593(25)	4.140	0.436		0.011(36)
				FB	3.583(25)				0.001(36)
${}^{56}\text{Fe}$	3pG	3.733(14)	3.654(14)	2pF	3.657(11)	4.143(15)	0.472(2)		0.003(18)
				3pG	3.654(12)	3.584(11)	2.201(10)	0.486(26)	0.000(18)
${}^{56}\text{Fe}$	2pF	3.720(52)	3.641(52)	2pF	3.640(41)	4.113(36)	0.474(17)		-0.001(66)
${}^{56}\text{Fe}^2$	2pF	3.800(15)	3.723(15)	2pF	3.691(9)	4.146(11)	0.489(2)		-0.032(17)
${}^{56}\text{Fe}$	FB	3.714(24)	3.635(24)	2pF	3.643(24)	4.157	0.458		0.008(34)
				FB	3.635(24)				0.000(34)
${}^{58}\text{Fe}^2$	2pF	3.783(19)	3.707(19)	2pF	3.668(12)	4.057(16)	0.509(2)		-0.039(22)
${}^{58}\text{Fe}$	3pG	3.771(14)	3.694(14)	2pF	3.697(12)	4.176(16)	0.482(1)		0.003(18)
				3pG	3.694(12)	3.656(9)	2.231(9)	0.420(25)	0.000(18)
${}^{58}\text{Fe}$	FB	3.747(25)	3.669(25)	2pF	3.682(25)	4.194	0.466		0.012(36)
				FB	3.670(25)				0.001(36)
${}^{59}\text{Co}$	2pF	3.803(44)	3.726(44)	2pF	3.726(35)	4.074(51)	0.533(0)		0.00(5)
${}^{59}\text{Co}^1$	3pG	3.629(12)	3.548(12)	2pF	3.554(9)	3.947(11)	0.488(2)		0.006(15)
				3pG	3.566(20)	2.574(50)	2.266(12)	0.688(50)	0.018(23)
${}^{59}\text{Co}^2$	2pF	3.865(17)	3.790(17)	2pF	3.757(13)	4.192(18)	0.509(1)		-0.033(21)
${}^{59}\text{Co}$	FB	3.788(5)	3.711(5)	2pF	3.714(5)	4.222	0.474		0.003(7)
				FB	3.711(5)				0.000(7)
${}^{58}\text{Ni}^3$	3pF	3.764	3.685	2pF	3.685	4.219	0.458		0.000
				3pF	3.684	4.245	0.457	-0.033	-0.001
${}^{58}\text{Ni}$	FB	3.769(13)	3.690(13)	2pF	3.689(13)	4.201	0.467		-0.001(19)
				FB	3.689(13)				-0.001(19)

(continued)

TABLE III – (*continued*)

Nucleus	ρ_c	$\langle r^2 \rangle_c^{1/2}$ (fm)	${}^1\langle r^2 \rangle_p^{1/2}$ (fm)	ρ_p	${}^2\langle r^2 \rangle_p^{1/2}$ (fm)	c or a (fm)	z or α (fm)	w	$\Delta\langle r^2 \rangle_p^{1/2}$ (fm)
${}^{58}\text{Ni}$	FB	3.742(24)	3.662(24)	2pF	3.672(24)	4.235	0.444		0.009(34)
				FB	3.663(24)				0.001(34)
${}^{58}\text{Ni}$	SOG	3.772(4)	3.693(4)	2pF	3.696(4)	4.229	0.460		0.003(6)
				FB	3.695(4)				0.002(6)
${}^{60}\text{Ni}^3$	3pF	3.796	3.719	2pF	3.725	4.260	0.465		0.006
				3pF	3.719	4.466	0.461	-0.234	0.000
${}^{60}\text{Ni}$	3pG	3.796(14)	3.719(14)	2pF	3.721(11)	4.252(15)	0.466(1)		0.002(18)
				3pG	3.718(12)	3.767(9)	2.208(10)	0.441(26)	-0.001(18)
${}^{60}\text{Ni}$	FB	3.797(13)	3.719(13)	2pF	3.719(13)	4.243	0.468		0.000(19)
				FB	3.719(13)				0.000(19)
${}^{60}\text{Ni}$	FB	3.764(24)	3.686(24)	2pF	3.699(24)	4.278	0.442		0.013(34)
				FB	3.687(24)				0.001(34)
${}^{60}\text{Ni}$	FB	3.782(24)	3.704(24)	2pF	3.714(24)	4.269	0.455		0.010(34)
				FB	3.705(24)				0.001(34)
${}^{61}\text{Ni}^3$	3pF	3.807	3.730	2pF	3.733	4.243	0.476		0.003
				3pF	3.730	4.352	0.475	-0.131	0.000
${}^{62}\text{Ni}^3$	3pF	3.822	3.747	2pF	3.750	4.271	0.475		0.003
				3pF	3.747	4.396	0.473	-0.147	0.000
${}^{62}\text{Ni}$	3pG	3.833(14)	3.758(14)	2pF	3.760(12)	4.292(16)	0.472(1)		0.002(18)
				3pG	3.757(12)	3.814(8)	2.234(9)	0.423(26)	-0.001(18)
${}^{62}\text{Ni}$	2pF	3.827(29)	3.752(29)	2pF	3.751(22)	4.271(21)	0.475(8)		-0.001(36)
${}^{62}\text{Ni}$	FB	3.802(24)	3.726(24)	2pF	3.739(24)	4.318	0.450		0.013(34)
				FB	3.726(24)				0.000(34)
${}^{64}\text{Ni}$	2pF	3.906(24)	3.833(24)	2pF	3.822(21)	4.245(29)	0.524(3)		-0.011(32)
${}^{64}\text{Ni}^3$	3pF	3.845	3.771	2pF	3.775	4.330	0.466		0.004
				3pF	3.771	4.480	0.461	-0.174	0.000
${}^{64}\text{Ni}$	3pG	3.852(14)	3.778(14)	2pF	3.780(12)	4.349(16)	0.462(1)		0.002(18)
				3pG	3.778(12)	3.911(7)	2.218(9)	0.411(27)	0.000(18)
${}^{64}\text{Ni}^2$	FB	3.822(24)	3.747(24)	2pF	3.758(24)	4.370	0.439		0.011(34)
				FB	3.741(24)				-0.006(34)

(continued)

TABLE III – (*continued*)

Nucleus	ρ_c	$\langle r^2 \rangle_c^{1/2}$ (fm)	${}^1\langle r^2 \rangle_p^{1/2}$ (fm)	ρ_p	${}^2\langle r^2 \rangle_p^{1/2}$ (fm)	c or a (fm)	z or α (fm)	w	$\Delta\langle r^2 \rangle_p^{1/2}$ (fm)
${}^{63}\text{Cu}$	3pG	3.879(14)	3.804(14)	2pF	3.807(12)	4.308(17)	0.493(1)		0.003(18)
				3pG	3.803(12)	3.779(8)	2.291(9)	0.427(25)	-0.001(18)
${}^{63}\text{Cu}$	2pF	3.934(29)	3.859(29)	2pF	3.858(21)	4.162(20)	0.570(8)		-0.001(36)
${}^{63}\text{Cu}^2$	2pF	3.948(14)	3.873(14)	2pF	3.838(9)	4.249(12)	0.531(1)		-0.035(17)
${}^{63}\text{Cu}$	FB	3.885(5)	3.810(5)	2pF	3.813(5)	4.315	0.494		0.003(7)
				FB	3.809(5)				-0.001(7)
${}^{65}\text{Cu}$	3pG	3.895(14)	3.821(14)	2pF	3.824(13)	4.350(17)	0.487(1)		0.003(19)
				3pG	3.821(11)	3.875(6)	2.282(9)	0.394(25)	0.000(18)
${}^{65}\text{Cu}$	2pF	3.986(29)	3.914(29)	2pF	3.913(22)	4.154(30)	0.599(4)		-0.001(36)
${}^{65}\text{Cu}^2$	2pF	3.955(14)	3.882(14)	2pF	3.847(9)	4.282(13)	0.524(1)		-0.035(17)
${}^{65}\text{Cu}$	FB	3.905(5)	3.831(5)	2pF	3.833(5)	4.351	0.491		0.002(7)
				FB	3.830(5)				-0.001(7)
${}^{64}\text{Zn}$	2pF	3.966(18)	3.892(18)	2pF	3.890(15)	4.292(4)	0.544(8)		-0.002(23)
${}^{64}\text{Zn}$	3pG	3.927(14)	3.852(14)	2pF	3.856(12)	4.326(16)	0.513(1)		0.004(18)
				3pG	3.852(12)	3.736(10)	2.348(9)	0.433(24)	0.000(18)
${}^{64}\text{Zn}$	2pF	3.918(26)	3.843(26)	2pF	3.842(19)	4.303(20)	0.514(7)		-0.001(32)
${}^{64}\text{Zn}$	FB	3.899(23)	3.823(23)	2pF	3.833(23)	4.348	0.492		0.010(33)
				FB	3.824(23)				0.001(33)
${}^{66}\text{Zn}^2$	2pF	3.989(29)	3.916(29)	2pF	3.880(19)	4.315(25)	0.530(3)		-0.036(35)
${}^{66}\text{Zn}$	3pG	3.935(14)	3.861(14)	2pF	3.866(12)	4.346(17)	0.511(1)		0.005(18)
				3pG	3.861(12)	3.824(9)	2.345(9)	0.379(24)	0.000(18)
${}^{66}\text{Zn}$	2pF	3.952(23)	3.879(23)	2pF	3.878(19)	4.346(25)	0.518(3)		-0.001(30)
${}^{66}\text{Zn}^2$	FB	3.903(25)	3.829(25)	2pF	3.842(25)	4.366	0.491		0.014(36)
				FB	3.826(25)				-0.003(36)
${}^{68}\text{Zn}^2$	2pF	3.976(35)	3.904(35)	2pF	3.871(22)	4.382(28)	0.501(4)		-0.033(41)
${}^{68}\text{Zn}$	3pG	3.966(14)	3.893(14)	2pF	3.897(13)	4.412(17)	0.504(1)		0.004(19)
				3pG	3.893(12)	3.934(7)	2.340(9)	0.367(25)	0.000(18)

(continued)

TABLE III – (*continued*)

Nucleus	ρ_c	$\langle r^2 \rangle_c^{1/2}$ (fm)	${}^1\langle r^2 \rangle_p^{1/2}$ (fm)	ρ_p	${}^2\langle r^2 \rangle_p^{1/2}$ (fm)	c or a (fm)	z or α (fm)	w	$\Delta\langle r^2 \rangle_p^{1/2}$ (fm)
${}^{68}\text{Zn}$	2pF	3.958(36)	3.886(36)	2pF	3.885(28)	4.401(26)	0.501(11)		-0.001(46)
${}^{68}\text{Zn}$	FB	3.948(24)	3.875(24)	2pF	3.880(24)	4.421	0.491		0.005(34)
				FB	3.875(24)				0.000(34)
${}^{70}\text{Zn}$	2pF	4.045(18)	3.975(18)	2pF	3.973(14)	4.417(6)	0.544(7)		-0.002(23)
${}^{70}\text{Zn}$	3pG	3.989(15)	3.918(15)	2pF	3.922(14)	4.459(19)	0.500(0)		0.004(21)
				3pG	3.918(12)	3.942(6)	2.343(9)	0.423(27)	0.000(19)
${}^{70}\text{Zn}$	2pF	3.994(30)	3.923(30)	2pF	3.922(25)	4.434(34)	0.509(4)		-0.001(39)
${}^{70}\text{Zn}$	FB	3.987(31)	3.916(31)	2pF	3.916(31)	4.450	0.500		0.000(44)
				FB	3.915(31)				-0.001(44)
${}^{70}\text{Ge}$	2pF	4.069(19)	3.997(19)	2pF	3.990(14)	4.465(18)	0.535(3)		-0.007(24)
${}^{70}\text{Ge}$	2pF	4.054(8)	3.982(8)	2pF	3.975(6)	4.457(37)	0.530(10)		-0.007(10)
${}^{70}\text{Ge}$	FB	4.043(2)	3.971(2)	2pF	3.971(2)	4.442	0.533		0.000(3)
				FB	3.971(2)				0.000(3)
${}^{72}\text{Ge}$	2pF	4.052(19)	3.981(19)	2pF	3.974(15)	4.476(25)	0.522(8)		-0.007(24)
${}^{72}\text{Ge}$	2pF	4.087(8)	4.017(8)	2pF	4.009(6)	4.473(7)	0.543(1)		-0.008(10)
${}^{72}\text{Ge}$	FB	4.060(2)	3.989(2)	2pF	3.990(2)	4.490	0.526		0.001(3)
				FB	3.989(2)				0.000(3)
${}^{74}\text{Ge}$	2pF	4.125(8)	4.057(8)	2pF	4.049(6)	4.479(7)	0.561(1)		-0.008(10)
${}^{74}\text{Ge}$	FB	4.075(2)	4.005(2)	2pF	4.007(2)	4.553	0.512		0.002(3)
				FB	4.005(2)				0.000(3)
${}^{76}\text{Ge}$	2pF	4.126(8)	4.058(8)	2pF	4.050(6)	4.575(7)	0.527(1)		-0.008(10)
${}^{76}\text{Ge}$	FB	4.081(2)	4.012(2)	2pF	4.013(2)	4.583	0.504		0.001(3)
				FB	4.012(2)				0.000(3)
${}^{74}\text{Se}^{\text{I}}$	2pF	4.081(14)	4.009(14)	2pF	4.006(15)	4.399(22)	0.567(0)		-0.003(21)
${}^{74}\text{Se}$	3pF	4.046(47)	3.974(47)	2pF	3.973(47)	4.421(67)	0.542(1)		-0.001(66)
				3pF	3.973(8)	4.406(72)	0.541(2)	0.018(6)	-0.001(66)

(continued)

TABLE III – (*continued*)

Nucleus	ρ_c	$\langle r^2 \rangle_c^{1/2}$ (fm)	${}^1\langle r^2 \rangle_p^{1/2}$ (fm)	ρ_p	${}^2\langle r^2 \rangle_p^{1/2}$ (fm)	c or a (fm)	z or α (fm)	w (fm)	$\Delta\langle r^2 \rangle_p^{1/2}$ (fm)
${}^{74}\text{Se}^1$	3pG	4.131(75)	4.060(75)	2pF	4.061(110)	4.640(139)	0.509(14)		0.001(133)
				3pG	4.060(10)	3.906(154)	2.426(9)	0.657(89)	0.000(76)
${}^{76}\text{Se}$	2pF	4.162(11)	4.092(11)	2pF	4.089(8)	4.483(9)	0.581(2)		-0.003(14)
${}^{76}\text{Se}$	3pF	4.153(36)	4.083(36)	2pF	4.081(30)	4.489(42)	0.575(4)		-0.002(47)
				3pF	4.083(51)	4.422(14)	0.572(3)	0.081(35)	0.000(47)
${}^{76}\text{Se}^1$	3pG	4.212(28)	4.143(28)	2pF	4.144(40)	4.699(54)	0.533(5)		0.001(49)
				3pG	4.143(18)	3.755(70)	2.508(3)	0.795(29)	0.000(33)
${}^{78}\text{Se}$	2pF	4.138(15)	4.069(15)	2pF	4.067(12)	4.598(17)	0.528(1)		-0.002(19)
${}^{78}\text{Se}$	3pF	4.123(36)	4.054(36)	2pF	4.052(32)	4.599(43)	0.519(3)		-0.002(48)
				3pF	4.053(24)	4.557(15)	0.520(4)	0.053(37)	-0.001(48)
${}^{78}\text{Se}^1$	3pG	4.196(33)	4.128(33)	2pF	4.128(45)	4.805(59)	0.480(6)		0.000(56)
				3pG	4.128(9)	4.165(47)	2.398(5)	0.669(44)	0.000(34)
${}^{80}\text{Se}$	2pF	4.124(10)	4.056(10)	2pF	4.053(8)	4.688(9)	0.484(2)		-0.003(13)
${}^{80}\text{Se}$	3pF	4.136(33)	4.068(33)	2pF	4.064(31)	4.686(43)	0.492(1)		-0.004(45)
				3pF	4.067(23)	4.535(14)	0.499(3)	0.202(41)	-0.001(45)
${}^{80}\text{Se}$	3pG	4.123(32)	4.054(32)	2pF	4.051(43)	4.812(55)	0.427(6)		-0.003(54)
				3pG	4.054(25)	4.208(44)	2.282(6)	0.778(40)	0.000(41)
${}^{82}\text{Se}$	2pF	4.117(12)	4.050(12)	2pF	4.047(9)	4.741(10)	0.458(2)		-0.003(15)
${}^{82}\text{Se}^3$	3pF	4.134	4.067	2pF	4.063	4.738	0.469		-0.004
				3pF	4.066	4.569	0.481	0.232	-0.001
${}^{82}\text{Se}^1$	3pG	4.180(36)	4.114(36)	2pF	4.111(47)	4.893(60)	0.428(6)		-0.003(59)
				3pG	4.114(8)	4.279(43)	2.308(9)	0.795(48)	0.000(37)
${}^{88}\text{Sr}$	3pG	4.264(12)	4.197(12)	2pF	4.192(20)	4.888(25)	0.484(5)		-0.005(23)
				3pG	4.195(9)	4.347(1)	2.426(2)	0.527(35)	-0.002(15)
${}^{88}\text{Sr}$	2pF	4.171(19)	4.103(19)	2pF	4.101(15)	4.850(9)	0.443(8)		-0.002(24)
${}^{88}\text{Sr}$	FB	4.197(6)	4.130(6)	2pF	4.136(6)	4.875	0.454		0.006(9)
				FB	4.130(6)				0.000(9)
${}^{89}\text{Y}^1$	2pF	4.254(65)	4.187(65)	2pF	4.183(50)	4.783(46)	0.522(20)		-0.004(82)

(continued)

TABLE III – (*continued*)

Nucleus	ρ_c	$\langle r^2 \rangle_c^{1/2}$ (fm)	${}^1\langle r^2 \rangle_p^{1/2}$ (fm)	ρ_p	${}^2\langle r^2 \rangle_p^{1/2}$ (fm)	c or a (fm)	z or α (fm)	w	$\Delta\langle r^2 \rangle_p^{1/2}$ (fm)
${}^{89}\text{Y}$	3pG	4.240(23)	4.173(23)	2pF	4.175(18)	4.850(22)	0.490(4)		0.002(29)
				3pG	4.172(10)	4.491(6)	2.401(20)	0.315(27)	-0.001(25)
${}^{89}\text{Y}$	2pF	4.270(20)	4.203(20)	2pF	4.201(16)	4.877(8)	0.494(8)		-0.002(26)
${}^{90}\text{Zr}$	3pG	4.274(13)	4.207(13)	2pF	4.208(20)	4.916(25)	0.482(3)		0.001(24)
				3pG	4.206(9)	4.502(10)	2.401(1)	0.404(24)	-0.001(16)
${}^{90}\text{Zr}$	3pG	4.284(35)	4.217(35)	2pF	4.219(29)	4.881(36)	0.504(5)		0.002(45)
				3pG	4.217(99)	4.501(7)	2.447(27)	0.316(37)	0.000(105)
${}^{90}\text{Zr}$	FB	4.258(8)	4.191(8)	2pF	4.196(8)	4.909	0.477		0.005(11)
				FB	4.191(8)				0.000(11)
${}^{91}\text{Zr}$	3pG	4.313(12)	4.246(12)	2pF	4.247(19)	4.929(24)	0.500(3)		0.001(22)
				3pG	4.246(16)	4.393(10)	2.464(1)	0.504(25)	0.000(20)
${}^{92}\text{Zr}$	3pG	4.298(13)	4.232(13)	2pF	4.234(20)	4.931(25)	0.491(3)		0.002(24)
				3pG	4.231(5)	4.520(10)	2.426(1)	0.386(24)	-0.001(14)
${}^{92}\text{Zr}$	FB	4.295(11)	4.229(11)	2pF	4.234(11)	4.937	0.489		0.006(16)
				FB	4.229(11)				0.000(16)
${}^{94}\text{Zr}$	3pG	4.333(14)	4.268(14)	2pF	4.271(20)	4.948(26)	0.507(3)		0.003(24)
				3pG	4.267(4)	4.556(10)	2.464(1)	0.343(24)	-0.001(15)
${}^{94}\text{Zr}$	FB	4.316(10)	4.250(10)	2pF	4.258(10)	4.939	0.503		0.008(14)
				FB	4.250(10)				0.000(14)
${}^{96}\text{Zr}^{\textcolor{blue}{1}}$	3pG	4.371(13)	4.307(13)	2pF	4.304(21)	4.995(24)	0.507(5)		-0.003(25)
				3pG	4.301(5)	4.614(9)	2.470(1)	0.347(24)	-0.006(14)
${}^{93}\text{Nb}^{\textcolor{blue}{1}}$	2pF	4.332(65)	4.266(65)	2pF	4.262(50)	4.894(47)	0.524(19)		-0.004(82)
${}^{93}\text{Nb}$	2pF	4.332(9)	4.266(9)	2pF	4.265(7)	4.966(4)	0.495(3)		-0.001(11)
${}^{92}\text{Mo}$	3pG	4.281(78)	4.213(78)	2pF	4.222(86)	4.913(111)	0.492(9)		0.009(116)
				3pG	4.211(5)	4.687(70)	2.378(58)	0.206(177)	-0.002(78)
${}^{92}\text{Mo}$	3pG	4.343(26)	4.276(26)	2pF	4.279(22)	4.944(30)	0.513(3)		0.003(34)
				3pG	4.276(4)	4.602(10)	2.482(17)	0.266(23)	0.000(26)
${}^{92}\text{Mo}$	FB	4.295(16)	4.227(16)	2pF	4.236(16)	4.972	0.475		0.009(23)
				FB	4.227(16)				0.000(23)

(continued)

TABLE III – (*continued*)

Nucleus	ρ_c	$\langle r^2 \rangle_c^{1/2}$ (fm)	${}^1\langle r^2 \rangle_p^{1/2}$ (fm)	ρ_p	${}^2\langle r^2 \rangle_p^{1/2}$ (fm)	c or a (fm)	z or α (fm)	w	$\Delta\langle r^2 \rangle_p^{1/2}$ (fm)
${}^{94}\text{Mo}$	FB	4.333(16)	4.266(16)	2pF	4.277(16)	4.998	0.489		0.010(23)
				FB	4.265(16)				-0.001(23)
${}^{96}\text{Mo}$	FB	4.364(16)	4.299(16)	2pF	4.310(16)	5.012	0.504		0.011(23)
				FB	4.299(16)				0.000(23)
${}^{98}\text{Mo}^{\text{2}}$	FB	4.388(16)	4.324(16)	2pF	4.340(16)	5.039	0.511		0.017(23)
				FB	4.320(16)				-0.004(23)
${}^{100}\text{Mo}$	FB	4.429(16)	4.366(16)	2pF	4.380(16)	5.085	0.515		0.013(23)
				FB	4.366(16)				0.000(23)
${}^{104}\text{Pd}$	FB	4.437(10)	4.373(10)	2pF	4.375(10)	5.186	0.466		0.003(14)
				FB	4.373(10)				0.000(14)
${}^{106}\text{Pd}$	FB	4.467(11)	4.404(11)	2pF	4.406(11)	5.202	0.479		0.003(16)
				FB	4.404(11)				0.000(16)
${}^{108}\text{Pd}$	FB	4.524(10)	4.462(10)	2pF	4.465(10)	5.261	0.491		0.002(14)
				FB	4.462(10)				0.000(14)
${}^{110}\text{Pd}$	2pF	4.639(23)	4.579(23)	2pF	4.577(18)	5.318(21)	0.537(5)		-0.002(29)
${}^{110}\text{Pd}$	FB	4.541(10)	4.479(10)	2pF	4.481(10)	5.280	0.493		0.002(14)
				FB	4.479(10)				0.000(14)
${}^{110}\text{Cd}$	2pF	4.583(19)	4.520(19)	2pF	4.519(15)	5.348(19)	0.486(3)		-0.001(24)
${}^{112}\text{Cd}$	2pF	4.613(21)	4.551(21)	2pF	4.550(17)	5.399(19)	0.483(5)		-0.001(27)
${}^{114}\text{Cd}$	2pF	4.635(21)	4.574(21)	2pF	4.573(17)	5.418(19)	0.489(5)		-0.001(27)
${}^{114}\text{Cd}$	2pF	4.631(23)	4.571(23)	2pF	4.569(18)	5.331(21)	0.526(5)		-0.002(29)
${}^{116}\text{Cd}$	2pF	4.641(21)	4.581(21)	2pF	4.580(17)	5.439(19)	0.483(5)		-0.001(27)
${}^{112}\text{Sn}$	2pF	4.655(26)	4.593(26)	2pF	4.588(21)	5.404(26)	0.505(4)		-0.005(33)
${}^{112}\text{Sn}$	3pG	4.586(6)	4.523(6)	2pF	4.525(10)	5.347(12)	0.490(2)		0.002(12)
				3pG	4.521(6)	5.041(2)	2.500(1)	0.299(13)	-0.002(8)
${}^{114}\text{Sn}$	3pG	4.602(6)	4.540(6)	2pF	4.538(10)	5.386(12)	0.481(2)		-0.002(12)
				3pG	4.538(4)	5.050(2)	2.499(1)	0.337(13)	-0.002(7)

(continued)

TABLE III – (*continued*)

Nucleus	ρ_c	$\langle r^2 \rangle_c^{1/2}$ (fm)	${}^1\langle r^2 \rangle_p^{1/2}$ (fm)	ρ_p	${}^2\langle r^2 \rangle_p^{1/2}$ (fm)	c or a (fm)	z or α (fm)	w	$\Delta\langle r^2 \rangle_p^{1/2}$ (fm)
${}^{116}\text{Sn}$	3pG	4.619(6)	4.557(6)	2pF	4.558(10)	5.418(12)	0.479(2)		0.001(12)
				3pG	4.556(4)	5.139(2)	2.484(1)	0.281(13)	-0.001(7)
${}^{116}\text{Sn}$	2pF	4.627(22)	4.565(22)	2pF	4.564(18)	5.377(21)	0.502(5)		-0.001(28)
${}^{116}\text{Sn}$	SOG	4.627(1)	4.565(1)	2pF	4.566(1)	5.441	0.472		0.001(1)
				FB	4.565(1)				0.000(1)
${}^{117}\text{Sn}$	3pG	4.626(6)	4.565(6)	2pF	4.563(10)	5.435(12)	0.474(2)		-0.002(12)
				3pG	4.563(4)	5.136(2)	2.485(1)	0.306(13)	-0.002(7)
${}^{118}\text{Sn}$	2pF	4.680(16)	4.620(16)	2pF	4.615(13)	5.441(18)	0.506(1)		-0.005(21)
${}^{118}\text{Sn}^2$	2pF	4.674(19)	4.614(19)	2pF	4.595(15)	5.467(20)	0.479(1)		-0.019(24)
${}^{118}\text{Sn}$	2pF	4.674(19)	4.614(19)	2pF	4.595(15)	5.467(20)	0.479(1)		-0.019(24)
${}^{118}\text{Sn}$	3pG	4.634(6)	4.574(6)	2pF	4.571(10)	5.454(12)	0.470(2)		-0.003(12)
				3pG	4.572(0)	5.149(2)	2.483(1)	0.315(13)	-0.002(6)
${}^{119}\text{Sn}$	3pG	4.639(8)	4.579(8)	2pF	4.577(10)	5.464(12)	0.468(1)		-0.002(13)
				3pG	4.577(20)	5.177(2)	2.477(4)	0.299(16)	-0.002(22)
${}^{120}\text{Sn}$	2pF	4.640(27)	4.580(27)	2pF	4.577(20)	5.339(24)	0.528(5)		-0.003(34)
${}^{120}\text{Sn}$	3pG	4.646(6)	4.586(6)	2pF	4.583(10)	5.475(12)	0.468(2)		-0.003(12)
				3pG	4.584(62)	5.186(2)	2.478(1)	0.301(13)	-0.002(62)
${}^{122}\text{Sn}$	3pG	4.659(6)	4.599(6)	2pF	4.590(9)	5.525(11)	0.446(2)		-0.009(11)
				3pG	4.597(21)	5.166(2)	2.472(1)	0.394(13)	-0.002(22)
${}^{124}\text{Sn}^2$	2pF	4.693(19)	4.635(19)	2pF	4.617(15)	5.515(20)	0.471(1)		-0.018(24)
${}^{124}\text{Sn}$	2pF	4.693(19)	4.635(19)	2pF	4.617(15)	5.515(20)	0.471(1)		-0.018(24)
${}^{124}\text{Sn}$	3pG	4.670(6)	4.611(6)	2pF	4.606(10)	5.526(12)	0.458(2)		-0.005(12)
				3pG	4.609(22)	5.225(2)	2.475(1)	0.320(13)	-0.002(23)
${}^{124}\text{Sn}$	SOG	4.677(1)	4.618(1)	2pF	4.618(1)	5.555	0.451		0.000(1)
				FB	4.619(1)				0.001(1)
${}^{138}\text{Ba}$	3pG	4.837(1)	4.780(1)	2pF	4.773(0)	5.768(0)	0.451(0)		-0.007(1)
				3pG	4.779(21)	5.406(0)	2.542(0)	0.392(0)	-0.001(21)
${}^{139}\text{La}$	2pF	4.849(65)	4.792(65)	2pF	4.776(48)	5.735(60)	0.472(8)		-0.016(81)

(continued)

TABLE III – (*continued*)

Nucleus	ρ_c	$\langle r^2 \rangle_c^{1/2}$ (fm)	${}^1\langle r^2 \rangle_p^{1/2}$ (fm)	ρ_p	${}^2\langle r^2 \rangle_p^{1/2}$ (fm)	c or a (fm)	z or α (fm)	w	$\Delta\langle r^2 \rangle_p^{1/2}$ (fm)
${}^{142}\text{Nd}$	3pF	4.920(9)	4.863(9)	2pF	4.846(12)	5.751(15)	0.513(2)		-0.017(15)
				3pF	4.860(23)	5.584(1)	0.545(1)	0.166(17)	-0.003(15)
${}^{142}\text{Nd}$	2pF	4.862(32)	4.804(32)	2pF	4.804(26)	5.790(25)	0.463(10)		0.00(4)
${}^{142}\text{Nd}$	2pF	4.993(39)	4.937(39)	2pF	4.936(31)	5.854(31)	0.525(12)		-0.001(50)
${}^{144}\text{Nd}$	2pF	4.926(5)	4.869(5)	2pF	4.861(3)	5.657(2)	0.566(1)		-0.008(6)
${}^{146}\text{Nd}$	2pF	4.970(5)	4.914(5)	2pF	4.906(3)	5.685(1)	0.582(1)		-0.008(6)
${}^{146}\text{Nd}$	2pF	4.992(41)	4.937(41)	2pF	4.936(33)	5.882(31)	0.511(13)		-0.001(53)
${}^{148}\text{Nd}$	2pF	5.002(8)	4.947(8)	2pF	4.938(5)	5.701(3)	0.595(3)		-0.009(9)
${}^{150}\text{Nd}$	2pF	5.047(11)	4.993(11)	2pF	4.984(8)	5.749(4)	0.602(4)		-0.009(14)
${}^{150}\text{Nd}$	2pF	5.014(40)	4.960(40)	2pF	4.959(32)	5.879(33)	0.528(11)		-0.001(51)
${}^{150}\text{Nd}^3$	2pF	4.948	4.893	2pF	4.891	5.920	0.458		-0.002
${}^{144}\text{Sm}^2$	FB	4.944(9)	4.886(9)	2pF	4.865(9)	5.998	0.388		-0.022(13)
				FB	4.891(9)				0.005(13)
${}^{148}\text{Sm}$	2pF	4.989(34)	4.933(34)	2pF	4.932(27)	5.783(28)	0.555(9)		-0.001(43)
${}^{148}\text{Sm}$	FB	4.977(8)	4.921(8)	2pF	4.922(8)	5.929	0.476		0.001(11)
				FB	4.921(8)				0.000(11)
${}^{148}\text{Sm}^2$	FB	5.003(6)	4.947(6)	2pF	4.927(6)	6.004	0.438		-0.020(9)
				FB	4.952(6)				0.005(9)
${}^{150}\text{Sm}^2$	FB	5.050(6)	4.995(6)	2pF	4.986(6)	5.922	0.525		-0.010(9)
				FB	5.008(6)				0.013(9)
${}^{152}\text{Sm}$	FB	5.100(8)	5.046(8)	2pF	5.046(8)	5.970	0.543		0.000(11)
				FB	5.047(8)				0.001(11)
${}^{152}\text{Sm}^2$	FB	5.087(6)	5.033(6)	2pF	5.010(6)	6.000	0.503		-0.023(9)
				FB	5.050(6)				0.017(9)
${}^{154}\text{Sm}$	FB	5.126(8)	5.073(8)	2pF	5.072(8)	5.988	0.552		-0.001(11)
				FB	5.074(8)				0.001(11)

(continued)

TABLE III – (*continued*)

Nucleus	ρ_c	$\langle r^2 \rangle_c^{1/2}$ (fm)	${}^1\langle r^2 \rangle_p^{1/2}$ (fm)	ρ_p	${}^2\langle r^2 \rangle_p^{1/2}$ (fm)	c or a (fm)	z or α (fm)	w	$\Delta\langle r^2 \rangle_p^{1/2}$ (fm)
${}^{154}\text{Gd}$	FB	5.125	5.070	2pF	5.076	6.016	0.542		0.005
				FB	5.070				0.000
${}^{158}\text{Gd}$	FB	5.172(6)	5.119(6)	2pF	5.119(6)	6.041	0.558		-0.001(9)
				FB	5.121(6)				0.002(9)
${}^{165}\text{Ho}^3$	2pF	5.23	5.182	2pF	5.175	6.210	0.513		-0.007
${}^{165}\text{Ho}^3$	2pF	5.19	5.140	2pF	5.133	6.149	0.515		-0.007
${}^{166}\text{Er}^2$	FB	5.227(20)	5.174(20)	2pF	5.179(20)	6.207	0.518		0.005(28)
				FB	5.171(20)				-0.003(28)
${}^{174}\text{Yb}^2$	FB	5.415(30)	5.365(30)	2pF	5.355(30)	6.420	0.534		-0.010(43)
				FB	5.368(30)				0.003(43)
${}^{175}\text{Lu}$	FB	5.367(30)	5.315(30)	2pF	5.312(30)	6.388	0.520		-0.003(43)
				FB	5.313(30)				-0.002(43)
${}^{184}\text{W}$	2pF	5.421(80)	5.370(80)	2pF	5.370(68)	6.527(72)	0.487(23)		0.00(10)
${}^{186}\text{W}$	2pF	5.400(41)	5.349(41)	2pF	5.349(35)	6.599(35)	0.424(14)		0.00(5)
${}^{192}\text{Os}$	FB	5.412(4)	5.362(4)	2pF	5.346(4)	6.514	0.475		-0.016(6)
				FB	5.361(4)				-0.001(6)
${}^{196}\text{Pt}$	FB	5.383(20)	5.333(20)	2pF	5.331(20)	6.529	0.454		-0.001(28)
				FB	5.333(20)				0.000(28)
${}^{197}\text{Au}$	2pF	5.327(64)	5.276(64)	2pF	5.269(53)	6.409(66)	0.475(8)		-0.007(83)
${}^{204}\text{Hg}$	FB	5.476(1)	5.426(1)	2pF	5.414(1)	6.685	0.425		-0.002(2)
				FB	5.428(1)				0.002(2)
${}^{203}\text{Ti}$	FB	5.464(5)	5.414(5)	2pF	5.412(5)	6.662	0.439		0.001(7)
				FB	5.414(5)				0.000(7)
${}^{205}\text{Ti}^3$	FB	5.470(5)	5.421(5)	2pF	5.421(5)	6.673	0.440		-0.001(7)
				FB	5.421(5)				0.000(7)
${}^{205}\text{Ti}^3$	SOG	5.479	5.430	2pF	5.423	6.670	0.443		-0.007
				FB	5.429				-0.001
${}^{204}\text{Pb}$	FB	5.480(2)	5.430(2)	2pF	5.429(2)	6.654	0.458		0.002(3)
				FB	5.430(2)				0.000(3)

(continued)

TABLE III – (*continued*)

Nucleus	ρ_c	$\langle r^2 \rangle_c^{1/2}$ (fm)	${}^1\langle r^2 \rangle_p^{1/2}$ (fm)	ρ_p	${}^2\langle r^2 \rangle_p^{1/2}$ (fm)	c or a (fm)	z or α (fm)	w	$\Delta\langle r^2 \rangle_p^{1/2}$ (fm)
${}^{206}\text{Pb}$	2pF	5.506(40)	5.457(40)	2pF	5.456(38)	6.629(49)	0.496(2)		-0.001(55)
${}^{206}\text{Pb}$	FB	5.491(2)	5.441(2)	2pF	5.443(2)	6.670	0.461		-0.003(3)
${}^{206}\text{Pb}$ ³	SOG	5.49	5.440	2pF	5.439	6.668	0.458		-0.001
				FB	5.440				0.000
${}^{207}\text{Pb}$	2pF	5.515(48)	5.466(48)	2pF	5.465(46)	6.639(59)	0.498(3)		-0.001(66)
${}^{207}\text{Pb}$	FB	5.497(2)	5.448(2)	2pF	5.445(2)	6.672	0.461		-0.004(3)
${}^{208}\text{Pb}$	FB	5.503(2)	5.454(2)	2pF	5.450(2)	6.682	0.459		0.000(3)
${}^{208}\text{Pb}$	FB	5.500(1)	5.450(1)	2pF	5.451(1)	6.681	0.460		-0.003(1)
				FB	5.449(1)				-0.001(1)
${}^{208}\text{Pb}$	SOG	5.503(2)	5.454(2)	2pF	5.451(2)	6.684	0.458		-0.003(3)
				FB	5.453(2)				-0.001(3)
${}^{209}\text{Bi}$	2pF	5.510(82)	5.461(82)	2pF	5.461(74)	6.768(77)	0.411(26)		0.00(11)
${}^{209}\text{Bi}$ ²	3pG	5.522(22)	5.473(22)	2pF	5.422(45)	6.703(43)	0.421(20)		-0.051(50)
				3pG	5.468(22)	6.393(1)	2.726(2)	0.372(62)	-0.005(31)
${}^{209}\text{Bi}$	FB	5.519(4)	5.469(4)	2pF	5.467(4)	6.719	0.450		0.007(6)
				FB	5.469(4)				0.000(6)
${}^{232}\text{Th}$ ³	2pF	5.645	5.598	2pF	5.594	6.878	0.459		-0.004

¹ Inconsistent data as listed in Table. I.² Data with insufficient q covered in experiments as listed in Table. II.³ No uncertainties were given in original references.

Table IV. Fourier-Bessel coefficients.

${}^1\langle r^2 \rangle_p^{1/2}$	rms point-proton radius calculated from $\langle r^2 \rangle_c^{1/2}$
${}^2\langle r^2 \rangle_p^{1/2}$	rms point-proton radius calculated from the deduced ρ_p
$\Delta\langle r^2 \rangle_p^{1/2}$	${}^2\langle r^2 \rangle_p^{1/2} - {}^1\langle r^2 \rangle_p^{1/2}$
a1...a17	List of the Fourier-Bessel coefficients a_ν , with $\nu = 1$ to 17
R_{cut}	The cutoff radius of ρ_p , beyond which the point-proton density is assumed to be identical to zero

TABLE IV: Fourier-Bessel Coefficients. Data marked with * means the original ρ_c is SOG.

Nucleus	^{12}C	^{12}C	^{12}C	$^{12}\text{C}^*$	^{15}N	^{15}N
$^1\langle r^2 \rangle_p^{1/2}$ (fm)	2.348(15)	2.339(12)	2.354(5)	2.345(6)	2.497(9)	2.499(9)
$^2\langle r^2 \rangle_p^{1/2}$ (fm)	2.346(15)	2.339(12)	2.353(5)	2.346(6)	2.496(9)	2.499(9)
$\Delta\langle r^2 \rangle_p^{1/2}$ (fm)	-0.002(22)	0.000(17)	-0.001(8)	0.001(8)	-0.001(13)	0.000(13)
a1	1.596563e-02	1.598004e-02	1.595297e-02	2.281975e-02	2.599638e-02	2.599241e-02
a2	4.115996e-02	4.133531e-02	4.103032e-02	5.136918e-02	5.468020e-02	5.469316e-02
a3	4.212352e-02	4.244053e-02	4.167720e-02	3.926107e-02	3.537719e-02	3.539854e-02
a4	1.855897e-02	1.871583e-02	1.808079e-02	3.571197e-03	-7.424451e-03	-7.438440e-03
a5	-6.190735e-03	-6.413033e-03	-6.383995e-03	-1.771289e-02	-2.493136e-02	-2.491100e-02
a6	-1.611385e-02	-1.657838e-02	-1.622396e-02	-1.637021e-02	-1.419855e-02	-1.435063e-02
a7	-1.328560e-02	-1.324473e-02	-1.282481e-02	-7.016646e-03	-5.401176e-03	-5.177853e-03
a8	-6.299771e-03	-6.569263e-03	-6.170953e-03	-1.698104e-03	-1.316962e-03	-1.098842e-03
a9	-1.726897e-03	-2.098014e-03	-1.540239e-03	-3.723297e-04		
a10	2.335173e-04	2.175797e-04	-8.927504e-04	7.794712e-04		
a11	7.194713e-04	4.149610e-04	-6.668794e-04	1.570835e-03		
a12	3.514963e-04	-1.726156e-04	5.821748e-04	1.151321e-03		
a13	2.866935e-04	-2.814502e-05	-2.722491e-04			
a14	9.609303e-05	6.350011e-05	1.052738e-04			
a15	1.856198e-05	-3.820307e-05	-3.620588e-05			
a16	6.520046e-06		1.135163e-05			
a17			-3.277771e-06			
R_{cut} (fm)	8.0	8.0	8.0	7.0	7.0	7.0

Nucleus	^{16}O	$^{16}\text{O}^*$	$^{24}\text{Mg}^*$	^{26}Mg	^{27}Al	^{28}Si
${}^1\langle r^2 \rangle_p^{1/2}$ (fm)	2.625(8)	2.598	2.927	2.862(4)	2.937(2)	2.986(17)
${}^2\langle r^2 \rangle_p^{1/2}$ (fm)	2.628(8)	2.597	2.927	2.862(4)	2.936(2)	2.986(17)
$\Delta\langle r^2 \rangle_p^{1/2}$ (fm)	0.003(11)	-0.001	0.000	0.000(5)	-0.001(2)	0.000(24)
a1	2.054637e-02	2.914617e-02	3.463227e-02	2.971836e-02	4.428937e-02	3.401273e-02
a2	4.760091e-02	5.647782e-02	6.037433e-02	5.889596e-02	6.519556e-02	6.326490e-02
a3	3.837557e-02	2.778930e-02	1.924068e-02	2.726175e-02	3.440602e-03	2.400862e-02
a4	4.431331e-03	-1.378297e-02	-1.991819e-02	-1.752891e-02	-3.173175e-02	-2.137867e-02
a5	-1.758502e-02	-2.337924e-02	-1.639629e-02	-2.246972e-02	-1.255088e-02	-2.145450e-02
a6	-1.702676e-02	-1.069532e-02	-1.411800e-03	-5.818969e-03	4.309743e-03	-1.537139e-03
a7	-6.562210e-03	9.608988e-04	2.623029e-03	3.743963e-03	2.444201e-03	6.413753e-03
a8	-9.490810e-04	3.272896e-03	1.826016e-03	3.250719e-03	3.477012e-04	1.350742e-03
a9	-2.565435e-03	-4.063177e-06	1.448918e-03	-2.320072e-04	-4.422203e-04	-1.086999e-03
a10	-8.380531e-04	-2.066841e-03	2.718820e-04	-4.471895e-04	2.364777e-04	3.981004e-04
a11	9.269518e-04	-1.211414e-03	-1.451154e-03	2.679222e-04	-9.267005e-05	-5.069579e-05
a12	-4.964851e-04	-9.952122e-05	-1.948824e-03	-9.177517e-05	2.708646e-05	-4.344608e-05
a13	2.328624e-04	1.326208e-04	-1.063502e-03	1.648929e-05		4.075372e-05
a14				6.570403e-07		-2.827182e-05
a15					-1.566440e-06	
a16						
a17						
R_{cut} (fm)	8.0	7.0	7.5	8.0	7.0	8.0

Nucleus	$^{28}\text{Si}^*$	^{29}Si	^{30}Si	^{30}Si	^{31}P	^{31}P
$^1\langle r^2 \rangle_p^{1/2}$ (fm)						
$^2\langle r^2 \rangle_p^{1/2}$ (fm)	3.056	2.983(17)	3.080(25)	3.101(13)	3.093(10)	3.097(5)
$\Delta\langle r^2 \rangle_p^{1/2}$	3.057	2.983(17)	3.080(25)	3.099(13)	3.092(10)	3.096(5)
(fm)	0.001	0.000(24)	0.000(36)	-0.002(18)	-0.001(14)	-0.001(7)
a1	3.365691e-02	3.403109e-02	2.877670e-02	2.870428e-02	3.584724e-02	3.582275e-02
a2	6.100640e-02	6.337192e-02	5.708663e-02	5.662182e-02	6.333583e-02	6.323283e-02
a3	2.185060e-02	2.352947e-02	2.829021e-02	2.772141e-02	1.973928e-02	1.970157e-02
a4	-2.112481e-02	-2.352680e-02	-1.577822e-02	-1.581504e-02	-2.435994e-02	-2.440411e-02
a5	-2.007345e-02	-2.358947e-02	-2.406060e-02	-2.340410e-02	-1.931094e-02	-1.877773e-02
a6	-2.052967e-03	-1.956243e-03	-7.250047e-03	-6.863818e-03	1.037494e-03	2.308588e-03
a7	5.133502e-03	5.373473e-03	4.430734e-03	5.779925e-03	6.801934e-03	7.048409e-03
a8	2.342732e-03	-1.525890e-04	3.069529e-03	4.615731e-03	1.895970e-03	1.448863e-03
a9	-4.902053e-04	-9.338247e-04	-7.364589e-04	9.983989e-04	-1.292787e-03	-8.716005e-04
a10	-1.700314e-03	5.682957e-04	1.393181e-04	5.867981e-04	6.166283e-04	5.903799e-04
a11	-2.367768e-03	-2.212257e-05	0.000000e+00	-8.912147e-04	-2.695010e-04	-4.173896e-04
a12	-1.717107e-03	5.742443e-05	-2.087785e-05	9.353538e-04	1.077349e-04	3.094568e-04
a13	-5.268889e-04		1.453235e-05	-9.054803e-04	-4.329455e-05	-2.393001e-04
a14	3.191184e-05					1.917220e-04
a15						-1.582329e-04
a16						
a17						
R_{cut} (fm)	8.0	8.0	8.5	8.5	8.0	8.0

Nucleus	^{32}S	^{32}S	$^{32}\text{S}^*$	^{34}S	^{36}S	^{40}Ar
$^1\langle r^2 \rangle_p^{1/2}$ (fm)	3.155(4)	3.134(5)	3.165	3.190(4)	3.190(6)	3.339(14)
$^2\langle r^2 \rangle_p^{1/2}$ (fm)	3.155(4)	3.132(5)	3.163	3.190(4)	3.189(6)	3.339(14)
$\Delta\langle r^2 \rangle_p^{1/2}$ (fm)	0.000(5)	-0.002(7)	-0.002	0.000(5)	-0.001(8)	0.000(20)
a1	3.782632e-02	3.794495e-02	3.249026e-02	3.759484e-02	3.757796e-02	3.080704e-02
a2	6.402472e-02	6.473672e-02	6.177866e-02	6.209099e-02	6.140773e-02	5.795718e-02
a3	1.687779e-02	1.719937e-02	2.653505e-02	1.378933e-02	1.143655e-02	2.239808e-02
a4	-2.321547e-02	-2.372906e-02	-1.794419e-02	-2.395507e-02	-2.488865e-02	-2.009017e-02
a5	-1.480129e-02	-1.455381e-02	-1.914384e-02	-1.185839e-02	-9.489573e-03	-1.792485e-02
a6	5.021319e-03	5.127808e-03	-4.303782e-04	7.429517e-03	1.003871e-02	-6.388636e-05
a7	6.801478e-03	7.559575e-03	7.909112e-03	5.412630e-03	7.148188e-03	1.545077e-03
a8	-9.082013e-05	2.862724e-03	4.383320e-03	-1.179346e-03	-1.232658e-03	-7.950339e-04
a9	-2.639924e-04	-3.173820e-04	-8.243382e-05	7.447025e-05	-3.420397e-04	2.676228e-04
a10	3.000842e-04	-2.165358e-03	-1.180281e-03	1.905913e-04	5.016711e-04	-5.161040e-05
a11	-2.026076e-04	-6.786618e-04	-1.042131e-04	-1.645729e-04	-3.187245e-04	-1.318334e-05
a12	1.075008e-04	2.645798e-04	5.601718e-04	9.411380e-05	1.545170e-04	2.191645e-05
a13	-4.862096e-05	-6.385189e-04	3.471603e-04	-4.416611e-05	-6.344142e-05	-1.590001e-05
a14	1.939524e-05	6.686081e-04	4.816127e-05	1.807064e-05	2.288235e-05	8.891244e-06
a15	-6.940275e-06	-4.968635e-04	-4.009035e-05	-6.609234e-06	-7.368835e-06	-4.484961e-06
a16						
a17						
R_{cut} (fm)	8.0	8.0	8.5	8.0	8.0	9.0

Nucleus	$^{39}\text{K}^*$	^{40}Ca	$^{40}\text{Ca}^*$	^{48}Ca	$^{48}\text{Ca}^*$	^{48}Ti
$^1\langle r^2 \rangle_p^{1/2}$ (fm)	3.340	3.362(10)	3.393(3)	3.370(9)	3.379	3.516(1)
$^2\langle r^2 \rangle_p^{1/2}$ (fm)	3.341	3.362(10)	3.394(3)	3.370(9)	3.380	3.515(1)
$\Delta\langle r^2 \rangle_p^{1/2}$ (fm)	0.001	0.000(14)	0.001(4)	0.000(13)	0.001	-0.001(1)
a1	4.347822e-02	4.554013e-02	3.397428e-02	4.542292e-02	4.536497e-02	2.811708e-02
a2	6.460674e-02	6.517030e-02	6.241962e-02	6.298636e-02	6.315868e-02	5.756767e-02
a3	2.881319e-03	-1.924672e-03	2.123111e-02	-8.410696e-03	-7.660866e-03	2.869154e-02
a4	-3.156528e-02	-3.316478e-02	-2.564650e-02	-3.674488e-02	-3.745994e-02	-1.982559e-02
a5	-5.873454e-03	-4.252134e-03	-2.054689e-02	-3.975087e-04	-9.202509e-04	-2.739512e-02
a6	1.336223e-02	1.409978e-02	4.848680e-03	1.740118e-02	1.766053e-02	-3.438404e-03
a7	7.677105e-03	6.810154e-03	1.217437e-02	5.696771e-03	5.735914e-03	1.178502e-02
a8	3.043518e-03	-1.100266e-03	4.859153e-03	-2.253491e-03	-2.366892e-03	5.978863e-03
a9	2.731311e-03	-1.068879e-03	-9.301446e-04	-4.658239e-04	-4.730832e-04	-1.324895e-03
a10	1.060994e-03	6.613761e-04	-1.109849e-03	1.726411e-04	6.858272e-04	2.414937e-04
a11	-2.179987e-04	9.933549e-05	7.052367e-04	-8.442666e-05	-4.321065e-04	-4.267119e-06
a12	-4.069032e-04	-8.332034e-05	1.167110e-03	3.690151e-05	-8.624713e-04	-1.649377e-05
a13	-2.142922e-04	3.783396e-05	5.618494e-04	-1.460134e-05	-4.314099e-04	
a14	-5.559765e-05	-1.412584e-05	8.957933e-05	5.258387e-06	-9.384891e-05	
a15	-8.174469e-06			-4.369301e-05	-1.730053e-06	-8.026836e-06
a16						
a17						
R_{cut} (fm)	8.0	8.0	9.0	8.0	8.0	10.0

Nucleus	^{50}Ti	$^{50}\text{Cr}^1$	$^{52}\text{Cr}^1$	$^{54}\text{Cr}^1$	^{54}Fe	^{56}Fe
$^1\langle r^2 \rangle_p^{1/2}$ (fm)	3.492(2)	3.581(4)	3.563(3)	3.611(4)	3.582(25)	3.635(24)
$^2\langle r^2 \rangle_p^{1/2}$ (fm)	3.490(2)	3.587(4)	3.570(3)	3.615(4)	3.583(25)	3.635(24)
$\Delta\langle r^2 \rangle_p^{1/2}$ (fm)	-0.002(2)	0.006(5)	0.007(4)	0.004(5)	0.001(36)	0.000(34)
a1	3.215388e-02	3.962133e-02	3.972388e-02	3.944157e-02	4.284514e-02	4.251579e-02
a2	6.101673e-02	6.482571e-02	6.546614e-02	6.314552e-02	6.756200e-02	6.532656e-02
a3	2.152733e-02	7.618844e-03	6.934007e-03	5.080074e-03	1.760707e-03	2.663486e-04
a4	-2.857098e-02	-3.630297e-02	-3.947223e-02	-3.678638e-02	-4.232862e-02	-3.935634e-02
a5	-2.403903e-02	-1.311235e-02	-1.408978e-02	-1.204605e-02	-1.343669e-02	-1.058378e-02
a6	4.793602e-03	1.310386e-02	1.560344e-02	1.376826e-02	1.798943e-02	1.609531e-02
a7	1.435131e-02	1.161340e-02	1.441065e-02	1.015703e-02	1.055464e-02	8.288705e-03
a8	6.874128e-03	-1.825840e-03	-4.651349e-04	-3.003864e-03	-2.350556e-03	-4.295403e-03
a9	-8.554219e-04	-5.649202e-03	-4.605148e-03	-1.712969e-03	3.070763e-04	-4.081146e-04
a10	2.998999e-04	-4.058091e-03	-3.144843e-03	1.996647e-03	2.756610e-05	9.776330e-04
a11		-2.281479e-03	-1.738650e-03	-1.058953e-03	-5.260867e-05	-7.159533e-04
a12					3.341614e-05	4.147227e-04
a13					-1.710908e-05	-2.145191e-04
a14					7.909983e-06	1.028631e-04
a15					-3.415155e-06	-4.642120e-05
a16					1.395883e-06	1.984173e-05
a17					-5.487390e-07	-8.058765e-06
R_{cut} (fm)	9.5	9.0	9.0	9.0	9.0	9.0

Nucleus	^{58}Fe	^{59}Co	^{58}Ni	^{58}Ni	$^{58}\text{Ni}^*$	^{60}Ni
$^1\langle r^2 \rangle_p^{1/2}$ (fm)	3.669(25)	3.711(5)	3.690(13)	3.662(24)	3.693(4)	3.719(13)
$^2\langle r^2 \rangle_p^{1/2}$ (fm)	3.670(25)	3.711(5)	3.689(13)	3.663(24)	3.695(4)	3.719(13)
$\Delta\langle r^2 \rangle_p^{1/2}$ (fm)	0.001(36)	0.000(7)	-0.001(18)	0.001(34)	0.002(5)	0.000(18)
a1	4.227483e-02	4.364114e-02	4.542231e-02	4.557003e-02	5.195915e-02	4.520016e-02
a2	6.338518e-02	6.416929e-02	6.790913e-02	6.821116e-02	6.586682e-02	6.610298e-02
a3	-1.660283e-03	-3.608071e-03	-3.101441e-03	-3.651049e-03	-1.802876e-02	-4.751480e-03
a4	-3.735839e-02	-3.920587e-02	-4.455637e-02	-4.362350e-02	-4.132518e-02	-4.180750e-02
a5	-7.655770e-03	-6.555865e-03	-9.554412e-03	-8.960143e-03	4.071859e-03	-6.440688e-03
a6	1.568331e-02	1.703081e-02	2.026865e-02	1.960069e-02	2.023399e-02	1.900107e-02
a7	6.988238e-03	9.332996e-03	1.125435e-02	8.636691e-03	4.359107e-03	9.186037e-03
a8	-5.600399e-06	6.075592e-04	-2.751796e-03	-4.058289e-03	-4.329121e-03	-2.732555e-03
a9	1.208685e-03	-1.582971e-04	-2.297455e-03	2.922737e-04	-6.918623e-04	-1.732915e-03
a10	-1.007581e-03	1.405334e-05	1.021351e-03	3.921843e-04	1.775114e-03	8.795505e-04
a11	6.254111e-04	-2.286697e-06	-4.300111e-04	-3.574384e-04	5.751400e-04	-4.043266e-04
a12	-3.407045e-04	7.116740e-06	1.740287e-04	2.217092e-04	-3.348418e-04	1.883321e-04
a13	1.710438e-04	-1.185289e-05	-6.548317e-05	-1.184905e-04	-3.345732e-04	-8.657926e-05
a14	-8.065395e-05	1.348735e-05	2.975297e-05	5.789479e-05	-1.427534e-04	2.949164e-05
a15	3.601894e-05	-1.132458e-05	-4.009274e-05	2.643947e-05	-2.297084e-05	-3.972763e-05
a16	-1.529401e-05	7.473739e-06			1.139609e-05	3.348999e-06
a17	6.181152e-06	-4.071306e-06			-4.650608e-06	-4.828065e-07
R_{cut} (fm)	9.0	9.0	9.0	9.0	8.5	9.0

Nucleus	^{60}Ni	^{60}Ni	^{62}Ni	$^{64}\text{Ni}^{\textcolor{blue}{1}}$	^{63}Cu	^{65}Cu
$^1\langle r^2 \rangle_p^{1/2}$ (fm)	3.686(24)	3.704(24)	3.726(24)	3.747(24)	3.810(5)	3.831(5)
$^2\langle r^2 \rangle_p^{1/2}$ (fm)	3.687(24)	3.705(24)	3.726(24)	3.741(24)	3.809(5)	3.830(5)
$\Delta\langle r^2 \rangle_p^{1/2}$ (fm)	0.001(34)	0.001(34)	0.000(34)	-0.006(34)	-0.001(7)	-0.001(7)
a1	4.538472e-02	4.527013e-02	4.510057e-02	4.496973e-02	4.613848e-02	4.597753e-02
a2	6.652640e-02	6.601390e-02	6.439329e-02	6.292853e-02	6.360731e-02	6.235324e-02
a3	-5.662318e-03	-5.536085e-03	-7.697912e-03	-1.018829e-02	-8.723592e-03	-1.052501e-02
a4	-4.143514e-02	-4.120692e-02	-3.970552e-02	-4.001176e-02	-3.796898e-02	-3.779939e-02
a5	-5.713106e-03	-5.836025e-03	-3.296697e-03	-6.959134e-04	-1.911211e-03	3.020420e-04
a6	1.896097e-02	1.902484e-02	1.874935e-02	1.938670e-02	1.624056e-02	1.652803e-02
a7	8.431918e-03	7.921799e-03	6.242866e-03	5.879437e-03	7.175426e-03	6.267175e-03
a8	-1.804360e-03	-1.638038e-03	-4.031390e-03	-4.160818e-03	-4.692072e-04	-1.249839e-03
a9	6.366733e-04	8.313381e-04	6.754621e-04	1.033736e-04	-6.751207e-04	-1.141211e-03
a10	-2.010803e-04	-3.940603e-04	1.501763e-04	6.571324e-04	6.260257e-04	1.138613e-03
a11	5.746601e-05	1.835792e-04	-2.381003e-04	-5.589264e-03	-3.959908e-04	-7.392937e-04
a12	1.331424e-05	-8.386650e-05	1.681101e-04	3.444653e-04	2.167442e-04	4.111728e-04
a13	-1.370223e-06	3.736103e-05	-9.566612e-05	-1.846391e-04	-1.089592e-04	-2.088288e-04
a14	9.896715e-07	-1.611215e-05	4.857217e-05	9.064175e-05	5.134434e-05	9.924609e-05
a15	9.525149e-07	6.728179e-06	-2.276425e-05	-4.159264e-05	-2.293196e-05	-4.447439e-05
a16	-5.682319e-07	-2.718623e-06	1.000510e-05	1.799285e-05	9.733542e-06	1.898629e-05
a17	-2.795390e-07	1.052998e-06	4.153065e-06	-7.382035e-06	-3.927254e-06	-7.700881e-06
R_{cut} (fm)	9.0	9.0	9.0	9.0	9.0	9.0

Nucleus	^{64}Zn	^{66}Zn	^{68}Zn	^{70}Zn	^{70}Ge	^{72}Ge
$^1\langle r^2 \rangle_p^{1/2}$ (fm)	3.823(23)	3.829(25)	3.875(24)	3.916(31)	3.971(2)	3.989(2)
$^2\langle r^2 \rangle_p^{1/2}$ (fm)	3.824(23)	3.826(25)	3.875(24)	3.915(31)	3.971(2)	3.989(2)
$\Delta\langle r^2 \rangle_p^{1/2}$ (fm)	0.001(33)	-0.003(36)	0.000(34)	-0.001(44)	0.000(2)	0.000(2)
a1	4.759588e-02	4.755670e-02	4.719818e-02	4.689987e-02	3.854705e-02	3.844216e-02
a2	6.449839e-02	6.389514e-02	6.158918e-02	5.977867e-02	6.262698e-02	6.159914e-02
a3	-9.998843e-03	-1.072417e-02	-1.360669e-02	-1.535406e-02	7.000757e-03	5.186830e-03
a4	-3.684871e-02	-3.652183e-02	-3.574146e-02	-3.586833e-02	-3.413056e-02	-3.468691e-02
a5	-1.042917e-03	-7.060767e-04	3.382339e-03	4.643790e-03	-1.204848e-02	-1.109233e-02
a6	1.490984e-02	1.437325e-02	1.509797e-02	1.486399e-02	1.213304e-02	1.324801e-02
a7	2.374474e-03	2.370305e-03	5.335735e-03	6.840799e-03	7.561921e-03	7.337414e-03
a8	-4.010085e-03	-1.368670e-03	-3.336291e-04	1.462817e-03	-2.627114e-03	-2.905147e-03
a9	7.908496e-04	4.661117e-04	-9.571101e-04	-2.244602e-03	-3.412277e-03	-3.009004e-03
a10	7.177890e-05	-1.260966e-04	8.746290e-04	1.568889e-03	-3.765906e-04	-2.168392e-04
a11	-1.965322e-04	2.222911e-05	-5.599383e-04	-9.028172e-04	-3.024286e-04	-1.219300e-04
a12	1.478875e-04	3.279842e-06	3.101583e-04	4.714829e-04	1.951063e-04	-4.618611e-06
a13	-8.632372e-05	-6.272293e-06	-1.573806e-04	-2.304547e-04	-1.051300e-04	2.282053e-05
a14	4.443389e-05	4.399541e-06	7.477155e-05	1.066926e-04	5.167430e-06	-1.749377e-05
a15	-2.100659e-05	-2.422254e-06	-3.358021e-05	-4.701712e-05	-2.391687e-05	1.006701e-05
a16	9.281179e-06	1.175946e-06	1.432047e-05	1.976824e-05		
a17	-3.098890e-06	-5.244028e-07	-5.807554e-06	-7.925528e-06		
R_{cut} (fm)	9.0	9.0	9.0	9.0	10.0	10.0

Nucleus	^{74}Ge	^{76}Ge	^{88}Sr	^{90}Zr	^{92}Zr	^{94}Zr
$^1\langle r^2 \rangle_p^{1/2}$ (fm)	4.005(2)	4.012(2)	4.130(6)	4.191(8)	4.229(11)	4.250(10)
$^2\langle r^2 \rangle_p^{1/2}$ (fm)	4.005(2)	4.012(2)	4.130(6)	4.191(8)	4.229(11)	4.250(10)
$\Delta\langle r^2 \rangle_p^{1/2}$ (fm)	0.000(2)	0.000(2)	0.000(8)	0.000(11)	0.000(15)	0.000(14)
a1	3.834233e-02	3.829970e-02	5.708150e-02	4.662302e-02	4.636760e-02	4.622108e-02
a2	6.048918e-02	6.002528e-02	5.763384e-02	6.414544e-02	6.236847e-02	6.145578e-02
a3	2.976200e-03	1.660314e-03	-3.692578e-02	-1.338610e-02	-1.449057e-02	-1.453191e-02
a4	-3.545776e-02	-3.673767e-02	-3.114379e-02	-4.274922e-02	-4.060408e-02	-3.841225e-02
a5	-1.019560e-02	-9.595041e-03	2.070933e-02	3.156215e-03	3.974682e-03	4.982994e-03
a6	1.404737e-02	1.538349e-02	1.106822e-02	2.097814e-02	1.889424e-02	1.747524e-02
a7	7.536844e-03	7.722211e-03	-9.188192e-03	-8.447194e-04	-1.262836e-03	-2.405147e-03
a8	-2.789995e-03	-2.952781e-03	-4.528916e-03	-1.044176e-02	-9.096449e-03	-9.696695e-03
a9	-2.708794e-03	-3.002385e-03	8.728218e-04	-2.382438e-03	-1.898399e-03	-3.042147e-03
a10	3.432664e-04	1.598059e-04	-5.872301e-04	8.073207e-04	5.881798e-04	1.202571e-04
a11	3.662704e-04	4.188483e-04	3.783223e-04	-4.214314e-04	-4.043277e-04	-6.092702e-05
a12	-2.140278e-04	-2.521293e-04	-2.168125e-04	1.571224e-04	2.032325e-04	1.120446e-04
a13	1.081296e-04	1.314426e-04	1.133471e-04	-1.730796e-05	-7.538477e-05	-1.066575e-04
a14	-5.004884e-05	-6.301858e-05	-5.511210e-05	-3.367375e-05	1.545302e-05	7.183284e-05
a15	2.182996e-05	2.850829e-05	2.519432e-05	3.911539e-05	4.791478e-06	-3.832882e-05
a16			-1.089071e-05			
a17			4.466111e-06			
R_{cut} (fm)	10.0	10.0	9.0	10.0	10.0	10.0

Nucleus	⁹² Mo	⁹⁴ Mo	⁹⁶ Mo	⁹⁸ Mo ¹	¹⁰⁰ Mo	¹⁰⁴ Pd
¹ $\langle r^2 \rangle_p^{1/2}$ (fm)	4.227(16)	4.266(16)	4.299(16)	4.324(16)	4.366(16)	4.373(10)
² $\langle r^2 \rangle_p^{1/2}$ (fm)	4.227(16)	4.265(16)	4.299(16)	4.320(16)	4.366(16)	4.373(10)
$\Delta \langle r^2 \rangle_p^{1/2}$ (fm)	0.000(22)	-0.001(22)	0.000(22)	-0.004(22)	0.000(22)	0.000(14)
a1	3.098536e-02	3.086412e-02	3.076239e-02	3.068550e-02	3.054627e-02	4.152979e-02
a2	6.148961e-02	6.037915e-02	5.952882e-02	5.868812e-02	5.752575e-02	6.481298e-02
a3	2.334881e-02	2.161981e-02	2.040004e-02	1.894219e-02	1.699471e-02	-2.271533e-03
a4	-3.210825e-02	-3.195330e-02	-3.141877e-02	-3.140961e-02	-3.180175e-02	-4.331657e-02
a5	-3.135557e-02	-2.940467e-02	-2.729121e-02	-2.547199e-02	-2.416081e-02	-5.392620e-03
a6	5.079051e-03	5.614998e-03	6.247289e-03	7.097433e-03	7.790335e-03	2.174538e-02
a7	1.959579e-02	1.778918e-02	1.639736e-02	1.516128e-02	1.488918e-02	5.267997e-03
a8	4.695107e-03	2.888085e-03	1.546692e-03	1.207815e-03	1.686191e-03	-9.084220e-03
a9	-1.026884e-02	-9.968551e-03	-1.013088e-02	-8.131345e-03	-6.338009e-03	-5.718694e-03
a10	-8.131063e-03	-6.433963e-03	-5.873017e-03	-4.258892e-03	-2.662505e-03	1.379159e-03
a11	9.272674e-04	1.474218e-03	1.784627e-03	1.417489e-03	1.508098e-03	3.632616e-03
a12	2.127694e-03	1.381509e-03	1.125755e-03	6.606499e-04	2.327095e-04	1.511749e-03
a13	-9.789731e-04	-1.015290e-03	-1.081938e-03	-7.792903e-04	-6.338063e-04	
a14	-4.187790e-04	-1.569064e-05	2.003726e-04	2.235303e-03	3.042342e-04	
a15	6.251830e-04	-3.947725e-04	2.420711e-04	1.370964e-04	3.127636e-05	
a16	-1.444467e-04	-2.066512e-04	-1.931372e-04	-1.817945e-04	-1.419571e-04	
a17	-2.917478e-04	-8.733626e-05	9.379482e-07	8.892644e-05	1.021388e-04	
R_{cut} (fm)	12.0	12.0	12.0	12.0	12.0	11.0

Nucleus	^{106}Pd	^{108}Pd	^{110}Pd	$^{116}\text{Sn}^*$	$^{124}\text{Sn}^*$	$^{144}\text{Sm}^1$
$^1\langle r^2 \rangle_p^{1/2}$ (fm)	4.404(11)	4.462(10)	4.479(10)	4.565(1)	4.618(1)	4.886(9)
$^2\langle r^2 \rangle_p^{1/2}$ (fm)	4.404(11)	4.462(10)	4.479(10)	4.565(1)	4.619(1)	4.891(9)
$\Delta\langle r^2 \rangle_p^{1/2}$ (fm)	0.000(15)	0.000(14)	0.000(14)	0.000(1)	0.001(1)	0.005(12)
a1	4.137188e-02	4.106493e-02	4.097561e-02	6.899015e-02	6.817262e-02	7.548876e-02
a2	6.367390e-02	6.129021e-02	6.058746e-02	4.043861e-02	3.541013e-02	2.729386e-02
a3	-3.200717e-03	-5.787408e-03	-6.564896e-03	-5.747236e-02	-5.918981e-02	-7.026464e-02
a4	-4.214550e-02	-4.092247e-02	-4.052263e-02	-2.648813e-03	2.235317e-03	1.234955e-02
a5	-4.259386e-03	-2.645883e-03	-2.096760e-03	3.001300e-02	2.901410e-02	2.486867e-02
a6	2.096266e-02	2.005782e-02	1.947694e-02	-9.331048e-03	-1.252691e-02	-1.813711e-02
a7	4.063007e-03	3.687753e-03	2.837584e-03	-1.112177e-02	-9.868878e-03	-6.462613e-03
a8	-8.781408e-03	-8.289686e-03	-8.328761e-03	2.799850e-03	3.780635e-03	-3.472963e-03
a9	-2.707365e-03	-3.455343e-03	-2.491436e-03	4.358680e-04	3.398852e-04	2.693322e-03
a10	4.384550e-03	2.027586e-03	3.133509e-03	-1.073731e-03	-8.524031e-04	-2.946864e-03
a11	2.921031e-03	5.061815e-04	6.955663e-04	6.307835e-04	7.014318e-04	-4.524552e-03
a12	4.150467e-05	-8.379280e-04	-1.052261e-03	1.780342e-04	1.380447e-04	
a13				4.106462e-05	3.271429e-05	
a14				-2.351546e-04	-2.454906e-04	
a15				-1.550445e-05	-2.839644e-05	
a16						
a17						
R_{cut} (fm)	11.0	11.0	11.0	9.0	9.0	9.25

Nucleus	^{148}Sm	$^{148}\text{Sm}^1$	$^{150}\text{Sm}^1$	^{152}Sm	$^{152}\text{Sm}^1$	^{154}Sm
${}^1\langle r^2 \rangle_p^{1/2}$ (fm)	4.921(8)	4.947(6)	4.995(6)	5.046(8)	5.033(6)	5.073(8)
${}^2\langle r^2 \rangle_p^{1/2}$ (fm)	4.921(8)	4.952(6)	5.008(6)	5.047(8)	5.050(6)	5.074(8)
$\Delta\langle r^2 \rangle_p^{1/2}$ (fm)	0.000(11)	0.005(8)	0.013(8)	0.001(11)	0.017(8)	0.001(11)
a1	7.121389e-02	7.459119e-02	7.397074e-02	5.654716e-02	7.320934e-02	5.630702e-02
a2	3.394128e-02	2.506559e-02	2.568809e-02	4.661842e-02	2.275933e-02	4.545102e-02
a3	-6.064289e-02	-6.535464e-02	-5.799521e-02	-4.336271e-02	-5.943398e-02	-4.337816e-02
a4	5.871558e-03	1.271592e-02	1.249307e-02	-2.066911e-02	1.159723e-02	-2.044715e-02
a5	2.580718e-02	2.201007e-02	1.982634e-02	2.503678e-02	2.090990e-02	2.415934e-02
a6	-1.213987e-02	-1.639238e-02	-1.372574e-02	6.505643e-03	-9.402343e-03	6.843739e-03
a7	-6.352906e-03	-2.934120e-03	3.041652e-03	-9.883164e-03	8.654119e-03	-8.778126e-03
a8	3.467213e-03	1.718829e-03	1.456761e-03	-3.073585e-03	-2.593756e-03	-3.747890e-03
a9	-1.021071e-03	2.083367e-03	2.141497e-03	2.792917e-03	-2.093478e-03	8.545233e-04
a10	-4.033010e-04	-3.101280e-03	-6.528588e-03			-5.628200e-03
a11			-4.981671e-03	-5.223002e-03		
a12						
a13						
a14						
a15						
a16						
a17						
R_{cut} (fm)	9.5	9.25	9.25	10.5	9.25	10.5

Nucleus	^{154}Gd	^{158}Gd	$^{166}\text{Er}^{\textcolor{blue}{1}}$	$^{174}\text{Yb}^{\textcolor{blue}{1}}$	^{175}Lu	^{192}Os
${}^1\langle r^2 \rangle_p^{1/2}$ (fm)	5.070	5.119(6)	5.174(20)	5.365(30)	5.315(30)	5.362(4)
${}^2\langle r^2 \rangle_p^{1/2}$ (fm)	5.070	5.121(6)	5.171(20)	5.368(30)	5.313(30)	5.361(4)
$\Delta\langle r^2 \rangle_p^{1/2}$ (fm)	0.000	0.002(8)	-0.003(28)	0.003(42)	-0.002(42)	-0.001(5)
a1	6.442225e-02	5.767503e-02	5.485308e-02	5.482275e-02	5.603736e-02	5.948057e-02
a2	3.834809e-02	4.448327e-02	4.859056e-02	4.123343e-02	4.351386e-02	4.273128e-02
a3	-5.226323e-02	-4.516590e-02	-4.132008e-02	-4.872458e-02	-4.811958e-02	-5.328530e-02
a4	-5.888588e-03	-1.956044e-02	-2.213074e-02	-2.352633e-02	-2.191630e-02	-1.143540e-02
a5	2.469187e-02	2.431282e-02	2.650956e-02	2.451196e-02	2.699652e-02	3.478904e-02
a6	-1.128790e-03	6.770923e-03	1.020063e-02	3.500804e-03	5.047266e-03	-7.411160e-03
a7	-7.125687e-03	-1.074815e-02	-7.503547e-03	-8.543717e-03	-1.023620e-02	-1.301689e-02
a8		-3.394482e-03	7.809361e-04	-2.479263e-04	4.962607e-04	5.619795e-03
a9		3.980999e-03	9.036106e-04	2.067865e-03	-4.140015e-04	4.963567e-03
a10			-6.814356e-04			4.678924e-04
a11			2.632456e-04			-3.650963e-03
a12						1.812840e-03
a13						
a14						
a15						
a16						
a17						
R_{cut} (fm)	10.0	10.5	11.0	11.0	11.0	11.0

Nucleus	^{196}Pt	^{204}Hg	^{203}Ti	^{205}Ti	$^{205}\text{Ti}^*$	^{204}Pb
${}^1\langle r^2 \rangle_p^{1/2}$ (fm)	5.333(20)	5.426(1)	5.414(5)	5.421(5)	5.430	5.430(2)
${}^2\langle r^2 \rangle_p^{1/2}$ (fm)	5.333(20)	5.428(1)	5.414(5)	5.421(5)	5.429	5.430(2)
$\Delta\langle r^2 \rangle_p^{1/2}$ (fm)	0.000(28)	0.002(2)	0.000(7)	0.000(7)	-0.001	0.000(2)
a1	5.052942e-02	5.118442e-02	5.188767e-02	5.183645e-02	7.577868e-02	5.242745e-02
a2	5.506466e-02	5.193619e-02	5.285239e-02	5.243914e-02	1.780112e-02	5.308675e-02
a3	-3.700815e-02	-4.201835e-02	-4.153893e-02	-4.180283e-02	-6.464683e-02	-4.142965e-02
a4	-3.814659e-02	-3.461087e-02	-3.400158e-02	-3.320597e-02	2.957895e-02	-3.226501e-02
a5	2.743065e-02	3.270222e-02	3.200764e-02	3.211366e-02	1.564746e-02	3.377158e-02
a6	1.781094e-02	1.312358e-02	1.341104e-02	1.292393e-02	-2.645869e-02	1.372434e-02
a7	-1.776232e-02	-2.191821e-02	-2.131844e-02	-2.103147e-02	6.101018e-03	-1.955237e-02
a8	-7.454417e-03	-4.642521e-03	-3.717038e-03	-3.860288e-03	8.127912e-03	-1.383473e-03
a9	8.949211e-03	1.104037e-02	9.345606e-03	1.118570e-02	-3.977856e-03	1.140204e-02
a10	2.622156e-03	1.243124e-03	3.404594e-04	1.444233e-03	5.115772e-05	4.371544e-04
a11	-2.136226e-03	-2.916103e-04	-3.505840e-04	-1.011263e-03	3.896471e-04	-1.207632e-03
a12	1.213492e-03	5.222655e-04	3.120854e-04	7.087514e-04	-2.136323e-03	9.249253e-04
a13	-1.233752e-04	-7.281229e-04	-2.238381e-04	-4.548544e-04	-1.028928e-03	-6.175981e-04
a14	-5.398346e-04	5.459359e-04	1.466322e-04	2.789588e-04	1.157232e-04	3.873314e-04
a15	7.398511e-04	-4.870410e-04	-9.091687e-05	-1.656082e-04	7.936150e-05	-2.330221e-04
a16			5.424354e-05	9.581157e-05	-9.872547e-06	1.361570e-04
a17			-3.135130e-05	-5.412224e-05	-6.280324e-07	-7.746030e-05
R_{cut} (fm)	12.0	12.0	12.0	12.0	10.0	12.0

Nucleus	^{206}Pb	$^{206}\text{Pb}^*$	^{207}Pb	^{208}Pb	^{208}Pb	$^{208}\text{Pb}^*$
$^1\langle r^2 \rangle_p^{1/2}$ (fm)	5.441(2)	5.440	5.448(2)	5.454(2)	5.450(1)	5.454(2)
$^2\langle r^2 \rangle_p^{1/2}$ (fm)	5.441(2)	5.440	5.447(2)	5.454(2)	5.449(1)	5.453(2)
$\Delta\langle r^2 \rangle_p^{1/2}$ (fm)	0.000(2)	0.000	-0.001(2)	0.000(2)	-0.001(1)	-0.001(2)
a1	5.234297e-02	7.654807e-02	5.230327e-02	5.225736e-02	6.319962e-02	7.635409e-02
a2	5.246954e-02	1.761205e-02	5.233215e-02	5.203080e-02	3.968508e-02	1.688965e-02
a3	-4.170539e-02	-6.362697e-02	-4.168733e-02	-4.189223e-02	-5.883590e-02	-6.362851e-02
a4	-3.132780e-02	3.185113e-02	-3.134633e-02	-3.110798e-02	-3.030298e-03	3.176930e-02
a5	3.359855e-02	1.623619e-02	3.373440e-02	3.363981e-02	3.711014e-02	1.554303e-02
a6	1.327156e-02	-2.402946e-02	1.282384e-02	1.227475e-02	-1.284376e-02	-2.534708e-02
a7	-1.947619e-02	8.662215e-03	-1.876857e-02	-1.923838e-02	-1.310369e-02	8.218625e-03
a8	-1.967891e-03	8.801736e-03	-6.797496e-04	-1.428475e-03	1.190236e-02	7.799320e-03
a9	1.238591e-02	-4.148119e-03	1.083945e-02	1.156311e-02	3.604900e-03	-3.993605e-03
a10	-7.375824e-05	-8.611480e-05	1.001287e-03	1.447201e-03	-3.447362e-03	3.116260e-04
a11	-1.896462e-03	4.785172e-04	-9.849215e-04	-2.892238e-03	1.629072e-04	4.758707e-04
a12	1.517677e-03	-2.095008e-03	7.142828e-04	2.881706e-04	7.941789e-04	-4.408392e-04
a13	-1.034998e-03	-1.059031e-03	-4.669960e-04	-2.053808e-04	-3.169106e-04	9.540242e-05
a14	6.535224e-04	9.666747e-05	2.890666e-04	1.323155e-04		7.839617e-05
a15	-3.952124e-04	7.414886e-05	-1.729276e-04	-8.162925e-05		3.636859e-06
a16	2.312767e-04	-1.160477e-05	1.005486e-04	4.856503e-05		9.345896e-06
a17	-1.318168e-04	-1.108092e-06	-5.708152e-05	-2.801781e-05		1.372124e-06
R_{cut} (fm)	12.0	10.0	12.0	12.0	11.0	10.0

Nucleus	
$^1\langle r^2 \rangle_p^{1/2}$ (fm)	^{209}Bi
$^2\langle r^2 \rangle_p^{1/2}$ (fm)	5.469(4)
$\Delta\langle r^2 \rangle_p^{1/2}$	5.469(4)
(fm)	0.000(5)
a1	5.277296e-02
a2	5.165831e-02
a3	-4.334622e-02
a4	-3.079738e-02
a5	3.443720e-02
a6	1.217190e-02
a7	-1.997960e-02
a8	-4.651801e-04
a9	1.232202e-02
a10	1.012790e-03
a11	-1.612628e-03
a12	5.606470e-04
a13	-2.693546e-04
a14	1.421720e-04
a15	-7.625756e-05
a16	4.113084e-05
a17	-2.209467e-05
R_{cut} (fm)	12.0

¹Data with large $\Delta\langle r^2 \rangle_p^{1/2}$ as listed in Tab. II.

-
- [1] H. Sakaguchi and J. Zenihiro, *Progress in Particle and Nuclear Physics* **97**, 1 (2017).
 - [2] S. Terashima, H. Sakaguchi, H. Takeda, T. Ishikawa, M. Itoh, T. Kawabata, T. Murakami, M. Uchida, Y. Yasuda, M. Yosoi, J. Zenihiro, H. P. Yoshida, T. Noro, T. Ishida, S. Asaji, and T. Yonemura, *Phys. Rev. C* **77**, 024317 (2008).
 - [3] J. Zenihiro, H. Sakaguchi, T. Murakami, M. Yosoi, Y. Yasuda, S. Terashima, Y. Iwao, H. Takeda, M. Itoh, H. P. Yoshida, and M. Uchida, *Phys. Rev. C* **82**, 044611 (2010).
 - [4] J. Zhang, B. Sun, I. Tanihata, R. Kanungo, C. Scheidenberger, S. Terashima, F. Wang, F. Ameil, J. Atkinson, Y. Ayyad, S. Bagchi, D. Cortina-Gil, I. Dillmann, A. Estradé, A. Evdokimov, F. Farinon, H. Geissel, G. Guastalla, R. Janik, S. Kaur, R. Knöbel, J. Kurcewicz, Y. Litvinov, M. Marta, M. Mostazo, I. Mukha, C. Nociforo, H. J. Ong, S. Pietri, A. Prochazka, B. Sitar, P. Strmen, M. Takechi, J. Tanaka, J. Vargas, H. Weick, and J. S. Winfield, *Science Bulletin* **69**, 1647 (2024).
 - [5] J. Zhao, B.-H. Sun, I. Tanihata, J. Xu, K. Zhang, A. Prochazka, L. Zhu, S. Terashima, J. Meng, L. He, C. Liu, G. Li, C. Lu, W. Lin, W. Lin, Z. Liu, P. Ren, Z. Sun, F. Wang, J. Wang, M. Wang, S. Wang, X. Wei, X. Xu, J. Zhang, M. Zhang, and X. Zhang, *Physics Letters B* **858**, 139082 (2024).
 - [6] S. Kaur, R. Kanungo, W. Horiuchi, G. Hagen, J. D. Holt, B. S. Hu, T. Miyagi, T. Suzuki, F. Ameil, J. Atkinson, Y. Ayyad, S. Bagchi, D. Cortina-Gil, I. Dillmann, A. Estradé, A. Evdokimov, F. Farinon, H. Geissel, G. Guastalla, R. Janik, R. Knöbel, J. Kurcewicz, Y. A. Litvinov, M. Marta, M. Mostazo, I. Mukha, C. Nociforo, H. J. Ong, T. Otsuka, S. Pietri, A. Prochazka, C. Scheidenberger, B. Sitar, P. Strmen, M. Takechi, J. Tanaka, I. Tanihata, S. Terashima, J. Vargas, H. Weick, and J. S. Winfield, *Phys. Rev. Lett.* **129**, 142502 (2022).
 - [7] J. D. Walecka, “Introduction,” in *Electron Scattering for Nuclear and Nucleon Structure*, Cambridge Monographs on Particle Physics, Nuclear Physics and Cosmology (Cambridge University Press, 2023).
 - [8] T. Suda and H. Simon, *Progress in Particle and Nuclear Physics* **96**, 1 (2017).
 - [9] J. Liu, R. Xu, J. Zhang, C. Xu, and Z. Ren, *Journal of Physics G: Nuclear and Particle Physics* **46**, 055105 (2019).
 - [10] H. De Vries, C. De Jager, and C. De Vries, *Atomic Data and Nuclear Data Tables* **36**, 495

(1987).

- [11] G. Fricke, C. Bernhardt, K. Heilig, L. Schaller, L. Schellenberg, E. Shera, and C. Dejager, *Atomic Data and Nuclear Data Tables* **60**, 177 (1995).
- [12] K. Tsukada, Y. Abe, A. Enokizono, T. Goke, M. Hara, Y. Honda, T. Hori, S. Ichikawa, Y. Ito, K. Kurita, C. Legris, Y. Maehara, T. Ohnishi, R. Ogawara, T. Suda, T. Tamae, M. Wakasugi, M. Watanabe, and H. Wauke, *Phys. Rev. Lett.* **131**, 092502 (2023).
- [13] T. Suda, “Electron Scattering Off Stable and Unstable Nuclei,” in *Handbook of Nuclear Physics*, edited by I. Tanihata, H. Toki, and T. Kajino (2023) pp. 1–24.
- [14] I. Sick, *Nuclear Physics A* **218**, 509 (1974).
- [15] B. Dreher, J. Friedrich, K. Merle, H. Rothhaas, and G. Luhrs, *Nucl. Phys. A* **235**, 219 (1974).
- [16] J. Cavedon, J. Bellicard, B. Frois, D. Goutte, M. Huet, P. Leconte, X.-H. Phan, S. Platchkov, and I. Sick, *Physics Letters B* **118**, 311 (1982).
- [17] J. W. Lightbody, S. Penner, S. P. Fivozinsky, P. L. Hallowell, and H. Crannell, *Phys. Rev. C* **14**, 952 (1976).
- [18] J. Ficenec, L. Fajardo, W. Trower, and I. Sick, *Physics Letters B* **42**, 213 (1972).
- [19] H. H. Xie and J. Li, *Phys. Rev. C* **110**, 064319 (2024).
- [20] H. H. Xie, J. Li, and H. Liang, *Phys. Rev. C* **109**, 034309 (2024).
- [21] H. H. Xie, J. Li, L. G. Jiao, and Y. K. Ho, *Phys. Rev. A* **107**, 042807 (2023).
- [22] H. Kurasawa and T. Suzuki, *Phys. Rev. C* **62**, 054303 (2000).
- [23] E. Tiesinga, P. J. Mohr, D. B. Newell, and B. N. Taylor, *Rev. Mod. Phys.* **93**, 025010 (2021).
- [24] H. Atac, M. Constantinou, Z.-E. Meziani, M. Paolone, and N. Sparveris, *Nature communications* **12**, 1759 (2021).
- [25] C. J. Horowitz and J. Piekarewicz, *Phys. Rev. C* **86**, 045503 (2012).
- [26] H. Gao and J. Zhou, *Few-Body Systems* **65**, 8 (2024).
- [27] P. Virtanen, R. Gommers, T. E. Oliphant, M. Haberland, T. Reddy, D. Cournapeau, E. Burovski, P. Peterson, W. Weckesser, J. Bright, S. J. van der Walt, M. Brett, J. Wilson, K. J. Millman, N. Mayorov, A. R. J. Nelson, E. Jones, R. Kern, E. Larson, C. J. Carey, İ. Polat, Y. Feng, E. W. Moore, J. VanderPlas, D. Laxalde, J. Perktold, R. Cimrman, I. Henriksen, E. A. Quintero, C. R. Harris, A. M. Archibald, A. H. Ribeiro, F. Pedregosa, P. van Mulbregt, and SciPy 1.0 Contributors, *Nature Methods* **17**, 261 (2020).
- [28] A. B. Jones and B. A. Brown, *Phys. Rev. C* **90**, 067304 (2014).

- [29] J. Zenihiro, H. Sakaguchi, S. Terashima, T. Uesaka, G. Hagen, M. Itoh, T. Murakami, Y. Nakatsugawa, T. Ohnishi, H. Sagawa, H. Takeda, M. Uchida, H. P. Yoshida, S. Yoshida, and M. Yosoi, “Direct determination of the neutron skin thicknesses in $^{40,48}\text{Ca}$ from proton elastic scattering at $e_p = 295$ mev,” (2018), arXiv:1810.11796 [nucl-ex] .
- [30] N. G. Shevchenko, A. A. Khomich, A. Y. Buki, V. N. Polishchuk, B. V. Mazan’ko, and Y. A. Kasatkin, Sov. J. Nucl. Phys. (Engl. Transl.); (United States) **27:2** (1978).
- [31] H. H. Xie, T. Naito, J. Li, and H. Liang, Physics Letters B **846**, 138232 (2023).